Comparison of the Effective Fragment Potential method with Symmetry-Adapted Perturbation Theory in the Calculation of Intermolecular Energies for Ionic Liquids

Samuel Tan
samuel.tan@monash.edu

Ekaterina Izgorodina
katya.pas@monash.edu

1 Introduction

Intermolecular interactions have an important effect on the physical and chemical properties of condensed chemical systems, especially where noncovalent interactions dominate. In ionic liquids (ILs), calculating the interacting energy not only requires accounting for the inherent covalent interactions and the ionic character that dictates much of the intermolecular dynamics, but also accurately including interactions such as hydrogen-bonding, π-π stacking, van der Waals forces, etc.[1–3] The noncovalent interactions in ionic liquids are often dominated by electrostatics (Coulomb), dispersion and induction (also known as polarization), as well as exchange-repulsion to a smaller extent. The complex interplay of all these interactions means that characterising the intermolecular dynamics of ionic liquids is a challenging task.[3]

Symmetry-adapted perturbation theory (SAPT) is the state-of-the-art method for calculating intermolecular interactions, and the separation of its components provides important insight into how the interactions affect the sturcture and properties of the chemical system in consideration.[4,5] However, while accurate, it is very expensive computationally. This theory often partitions the intermolecular interaction energy into electrostatic, exchange, induction and dispersion components. The charge-transfer is considered a part of the induction energy.

The general effective fragment potential (EFP) method was developed by Gordon et al.[6–10] as a computationally inexpensive method to model intermolecular interactions. This method was originally created to model solvents,[11–13] but has then been generalised.[14,15] It belongs to class of fragmentation methods, and is an *ab-initio* based method, without any empirical parameters, with each term developed independently of the rest. Each term in the EFP method represents an individual fundamental component of interaction energy such as electrostatics, exchange, polarization, dispersion and charge transfer. Thus it calculates the interaction energy as a sum of terms directly comparable with SAPT.

This work extends on the work done by Flick et al.,[16] who undertook a systematic study on the performance of EFP compared against a raft of semi-empirical and correlated methods. They used the S22 and S66 test sets of Hobza et al.[17,18] However, to date no systematic study has been done on the suitability of the EFP method for charged species like ionic liquids. While this method was not originally designed for charged species, its computational efficiency shows promise. This study attempts to identify how well EFP performs for ionic liquids in representing the intermolecular interactions. The test set is a suite of ionic liquids at various configurations, and the EFP data will be compared against the SAPT results. Three basis sets will be used for EFP to determine the accuracy gained when larger basis sets are used.

2 Theoretical Background

2.1 SAPT

Since Schrödinger's equation is a differential equation, mathematicians and physicists naturally turn to perturbation theory in their quest for solutions. It was first used by London et al.[19] to describe the intermolecular interaction operator as a multipole expansion. Since then, the theory has been improved and refined; the current benchmark for calculating the intermolecular interaction energy between two dimers [1] is symmetry-adapted perturbation theory.

The SAPT method has the Hamiltonian partitioned as

$$H = F_A + F_B + W_A + W_B + V$$

where F_A, F_B are the Fock operators for monomers A and B respectively. Similarly, W_A, W_B are the differences between the exact Coulomb operator and the Fock operator for each monomer. The V contains all the intermolecular terms. SAPT perturbs in all of W_A, W_B, V

[1] Note that the terms 'dimer' and 'monomer' refer to the chemical entities whose interaction with each other is of interest, as opposed to the usage in polymer chemistry.

when solving for the different energy components. The different energy components will be grouped as follows:

$$
\begin{aligned}
E_{\text{electrostatic}} &= E^{(10)}_{\text{elec,repl}} + E^{(12)}_{\text{elec,repl}} + E^{(13)}_{\text{elec,repl}} \\
E_{\text{exchange}} &= E^{(10)}_{\text{exch}} + E^{(11)}_{\text{exch}} + E^{(12)}_{\text{exch}} \\
E_{\text{induction}} &= E^{(20)}_{\text{ind,repl}} + E^{(30)}_{\text{ind,repl}} f E^{(22)}_{\text{ind}} + E^{(20)}_{\text{exch-ind,repl}} + \\
&\quad E^{(30)}_{\text{exch-ind,repl}} + E^{(22)}_{\text{exch-ind}} + \delta E^{(2)}_{\text{HF}} + \delta E^{(3)}_{\text{HF}} \\
E_{\text{dispersion}} &= E^{(20)}_{\text{disp}} + E^{(30)}_{\text{disp}} + E^{(21)}_{\text{disp}} + E^{(22)}_{\text{disp}} + E^{(20)}_{\text{exch-disp}} + \\
&\quad E^{(30)}_{\text{exch-disp}} + E^{(30)}_{\text{ind-disp}} + E^{(30)}_{\text{exch-ind-disp}} \\
E_{\text{charge-transfer}} &= E_{\text{ind}}(\text{dimer basis}) - E_{\text{ind}}(\text{monomer basis})
\end{aligned}
$$

The superscripts in parenthesis denote the perturbation orders of V and $W = W_A + W_B$ respectively. The SAPT charge-transfer energy is part of the SAPT induction energy when the dimer basis set is used. To extract the energy, the same calculation is performed in the monomer basis, i.e. where no charge-transfer is permitted, and the difference taken. The individual terms in this grouping are discussed in much more detail in references [20–25]. Reference [20] in particular provides a comprehensive review of the theory.

2.2 EFP

The EFP method partitions the interaction energy in the following way:

$$E_{\text{total interaction}} = E_{\text{elec}} + E_{\text{pol}} + E_{\text{disp}} + E_{\text{exch-repl}} + E_{\text{ct}}$$

In order, these are the electrostatic, polarization, dispersion, exchange-repulsion and charge-transfer components. These energies are derived from *ab-initio* methods: it uses Stone's distributed multipolar analysis[4] for the electrostatic and polarization terms. Polarization is also treated with static polarizability tensors. On the other hand, dynamic polarizability tensors are used to calculate the dispersion interaction. The exchange-repulsion is calculated using the Fock matrix. For more details of the method, look to references [7–9, 14, 15].

3 Results and Discussion

subsectionTheoretical procedures

3.0.1 Chemical systems studied

The chemical systems were all ionic liquid ion pairs. The anion is one of the eight anions included in this study: tetrafluoroborate, bromide, chloride, dicyanamide, mesylate, tosylate, hexafluorophosphate and bis{(trifluoromethyl)sulfonyl}amide. The cations used are based on methyl pyrrolidinium and methyl imidazolium. The length of the alkyl chain on the cation was varied, e.g. from dimethyl imidazolium to 1-butyl-3-methyl-imidazolium. The bulk of the cation is varied thus, and provides some insight into how the size of the cation affects the different energy components. The names and abbreviations of the different cations and anions, eight each, are tabulated in table 1.

Cations	abbreviation	Anions	abbreviation
dimethyl-imidazolium	C_1mim^+	tetrafluoroborate	BF_4^-
1-methyl-3-ethyl-imidazolium	C_2mim^+	bromide	Br^-
1-methyl-3-propyl-imidazolium	C_3mim^+	chloride	Cl^-
1-methyl-3-butyl-imidazolium	C_4mim^+	dicyanamide	Dca^-
dimethyl-pyrrolidinium	C_1mpyr^+	mesylate	Mes^-
1-ethyl-1-methyl-pyrrolidinium	C_2mpyr^+	bis{(trifluoromethyl)sulfonyl}amide	NTf_2^-
1-propyl-1-methyl-pyrrolidinium	C_3mpyr^+	hexafluorophosphate	PF_6^-
1-butyl-1-methyl-pyrrolidinium	C_4mpyr^+	tosylate	Tos^-

Table 1: List of cations and anions

Besides the different possible combinations between ion pairs, different configurations of these ion pairs were studied as well. These configurations are differentiated by how the anion interacts with the cation. Both cations are ring systems; if the anion approaches the cation from above, this is referred to as the above-plane configuration (shortened to p1). If the anion interacts with the cation in the plane of the ring, i.e. from the side, then this is referred to as an in-plane interaction. In-plane configurations are p2 and p3. The below-plane configuration is very much similar to the above-plane configuration; this is designated as p4. The different configurations for [C_3mim][Br] are presented in figure 1 as an example.

The NTf_2^- anion has different configurations, as shown in figure 2. This is because it can interact with the cation either through the nitrogen on the ring, or the oxygens on the sulfonyl groups. The above-plane configurations for this anion are p1 and p2; p1 is where the nitrogen faces the ring, and p2 is where the oxygens

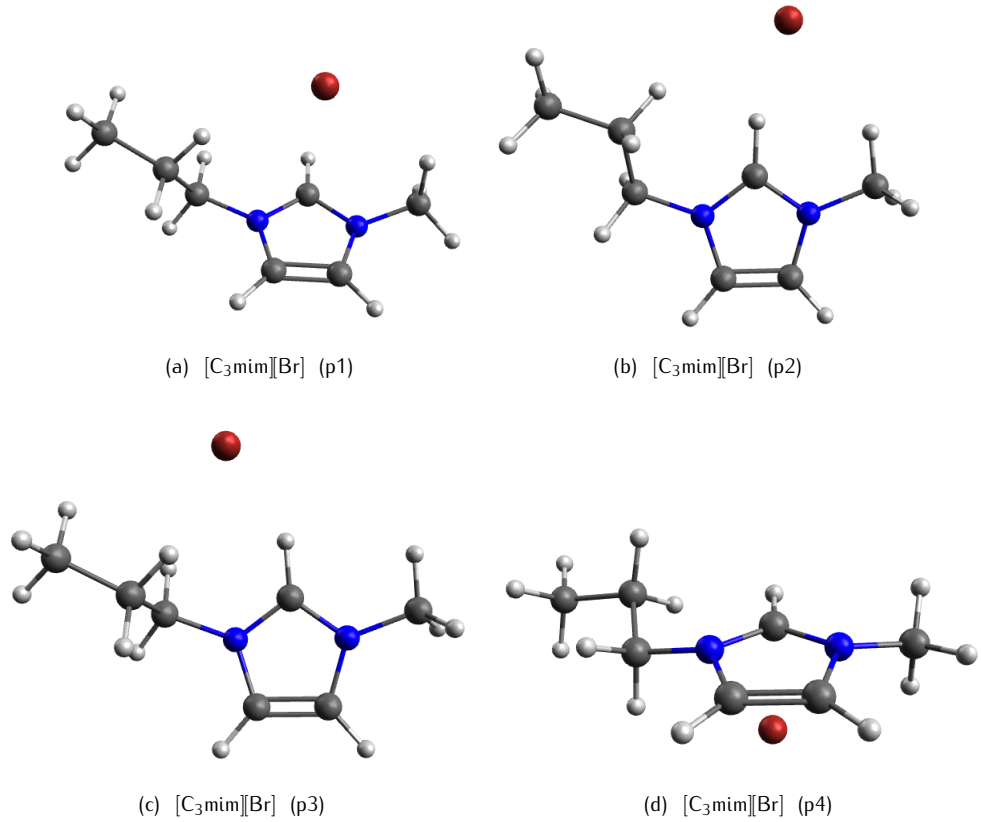

(a) [C_3mim][Br] (p1) (b) [C_3mim][Br] (p2)

(c) [C_3mim][Br] (p3) (d) [C_3mim][Br] (p4)

Figure 1: Different configurations of [C_3mim][Br]

face the ring. The next two configurations, p3 and p4, are where the nitrogen approaches the ring obliquely from below and from the side, respectively. The p5 and p6 configurations are the same as p3 and p4, with the oxygens approaching the ring from below, and side-on.

3.0.2 SAPT

The Psi4 quantum chemistry package was used for the SAPT calculations.[5] All SAPT calculations were performed at the SAPT2+3 level of theory,using the aug-cc-pVDZ basis set. There are some differences between this study and the work done by Flick et al. In the first place, they used the SAPT2+(3) level of theory, which does not include the $E^{(30)}_{\text{exch-disp}}$, $E^{(30)}_{\text{ind-disp}}$, and $E^{(30)}_{\text{exch-ind-disp}}$ terms. These terms belong to the dispersion interaction, and brings the intermolecular perturbation order to 3 for all components. Another difference is that this study considers the charge-transfer energy; this effectively doubles the computational expense, since for each chemical system the same calculation is performed twice, in both the dimer and monomer basis.

3.0.3 EFP

In the EFP method, the system is broken into fragments (typically each of the solvent molecules is a fragment). In this study, since only ion pairs are considered, there are only two fragments. These fragments are treated separately at an *ab-initio* level of theory. Then the cation and anion are allowed to interact and the interaction energy is decomposed into individual components.

Three basis sets were used for EFP: aug-cc-pVDZ, aug-cc-pVTZ and the Pople basis set 6-311++G**. [2] Three basis sets were used to see how consistent the method is between basis sets, and also the quality of the basis set that gives the best expense-to-error ratio.

3.0.4 SAPT and CCSD(T)/CBS

The CCSD(T)/CBS energies were also calculated for the ion pairs, and compared with the SAPT energies. For the total interaction energy, the statistics of the differences between the two methods are as follows: minimum -26.9 kJ·mol^{-1}, maximum = 25.7 kJ·mol^{-1}, mean -1.3 kJ·mol^{-1}, median -0.68 kJ·mol^{-1}, and standard deviation of 4.2 kJ·mol^{-1}. The outliers are [$C_{2,3}$mim][Dca] (p3): 7.47 & -13.1 kJ·mol^{-1}, [C_3im][PF_6] (p1): -12.0 kJ·mol^{-1}, [C_3pyr][Dca] (p3 & p4): 25.9 & -26.9 kJ·mol^{-1}.

Taking the difference between SAPT2+3 and the

[2] For the bromide anion, since it is not included in the 6-311++G** basis set, 6-311G** basis functions were used instead.

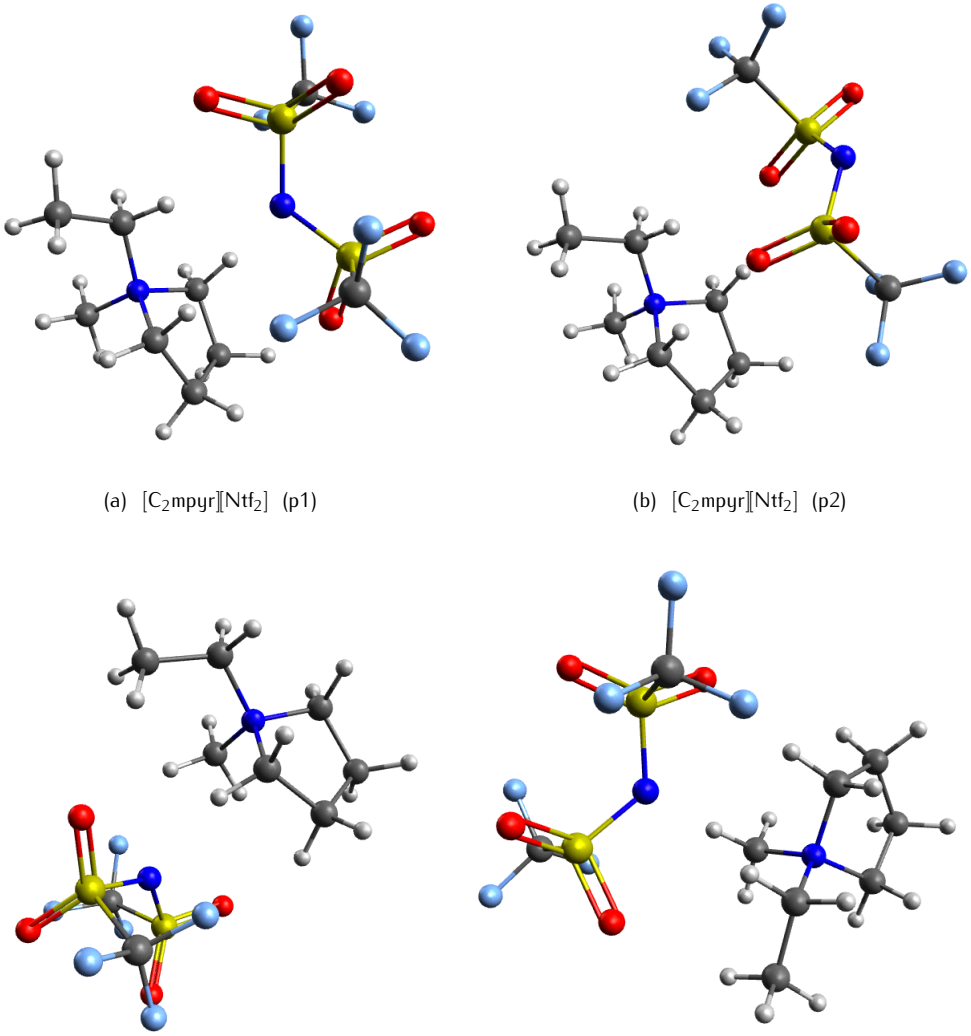

(a) $[C_2mpyr][Ntf_2]$ (p1)

(b) $[C_2mpyr][Ntf_2]$ (p2)

(c) $[C_2mpyr][Ntf_2]$ (p3)

(d) $[C_2mpyr][Ntf_2]$ (p4)

(e) $[C_2mpyr][Ntf_2]$ (p5)

(f) $[C_2mpyr][Ntf_2]$ (p6)

Figure 2: Different configurations of $[C_2mpyr][Ntf_2]$

SAPT Hartree–Fock energy, and comparing that difference with the correlation correction from CCSD(T)/CBS by subtracting the latter from the former, very good agreement is also shown. The minimum is -11.0 kJ·mol^{-1}, maximum 7.6 kJ·mol^{-1}, mean -2.3 kJ·mol^{-1}, median -1.5 kJ·mol^{-1}, and the standard deviation is 3.3 kJ·mol^{-1}. Outliers in this case are [$C_{2,3,4}$im][Cl] (p4): -9.17, -10.5 & -10.7 kJ·mol^{-1}, [$C_{3,4}$im][Br] (p4): -9.21 & -9.35 kJ·mol^{-1}and [C_3im][Dca] (p2 & p3) 7.56 & -11.0 kJ·mol^{-1}. The agreement between SAPT and CCSD(T)/CBS results validates the reliability of SAPT as a method to accurately determine the decomposition of the total interaction energy.

3.0.5 Basis sets

While three basis sets were used to give an indication of basis set dependency for the EFP method, only the aug-cc-pDVZ basis set was used for SAPT. There were some test calculations using a larger basis set, aug-cc-pVTZ, to determine whether aug-cc-pVDZ gave satisfactory accuracy. The difference between the two basis sets are tabulated in table 2. The calculations using aug-cc-pVTZ were run on some representative halide systems. Halides were selected because of smaller system sizes (monoatomic anions) and because they are more difficult to model. Due to the problematic nature of the charge-transfer interaction in the halides, the following discussion will ignore the differences in charge-transfer energies between the two basis sets.

One immediately observes the consistency between the two basis sets: with electrostatics, the triple zeta basis set always returns weaker energies (less negative), but correspondingly its exchange is less repulsive (less positive). The dispersion energy is also always stronger in the aug-cc-pVTZ basis set. While there is no such pattern in the difference in the induction energies, this is the interaction both basis sets agree best on, with absolute differences below 1 kJ·mol^{-1}. In the total interaction energy, the largest difference is 9 kJ·mol^{-1}. Considering the standard deviations, where these two basis sets differ, they differ *consistently* for each energetic component. This indicates that while they may not agree on the exact numbers, the trends between different chemical systems is well reflected. The fact that both basis sets showed such agreement for the halides, which are typically challenging, indicates that the aug-cc-pVTZ basis set would not provide much more insight and accuracy than the significantly less expensive aug-cc-pVDZ basis.

The aug-cc-pVTZ basis set requires tremendous amounts of time, in most cases more than double the amount of time required for the aug-cc-pVDZ basis set, which is already quite time consuming.

Name (Conf)	Electrostatics	Exchange	Induction	Dispersion	Total Energy	Charge-transfer
[C_1mim][Br] (p1)	4.77	-5.92	0.90	-7.05	-7.30	12.17
[C_1mim][Br] (p2)	1.42	-3.79	-0.20	-5.29	-7.87	7.45
[C_1mim][Cl] (p1)	4.23	-5.96	0.89	-6.61	-7.45	9.94
[C_1mim][Cl] (p2)	1.14	-4.27	-0.24	-5.62	-9.00	8.30
[C_2mim][Br] (p1)	4.43	-5.87	1.02	-6.83	-7.25	10.09
[C_2mim][Br] (p2)	1.66	-4.07	-0.04	-5.21	-7.66	7.64
[C_2mim][Br] (p1)	1.90	-4.17	0.13	-5.38	-7.51	7.10
[C_2mim][Br] (p2)	4.77	-5.93	1.00	-6.87	-7.03	11.73
[C_2mim][Cl] (p1)	3.92	-5.89	0.96	-6.41	-7.41	8.63
[C_2mim][Cl] (p2)	1.31	-4.42	-0.13	-5.49	-8.73	8.68
[C_2mim][Cl] (p3)	1.58	-4.56	0.10	-5.56	-8.45	7.81
[C_2mim][Cl] (p4)	4.25	-5.94	0.95	-6.40	-7.13	9.69
[C_3mpyr][Cl] (p1)	2.00	-4.61	0.90	-4.41	-6.11	6.49
[C_3mpyr][Cl] (p2)	1.71	-4.36	0.63	-4.29	-6.30	5.99
[C_3mpyr][Cl] (p3)	1.77	-4.50	0.75	-4.47	-6.44	
[C_4mim][Cl] (p1)	4.00	-5.93	1.06	-6.21	-7.08	8.33
[C_4mim][Cl] (p2)	1.40	-4.43	-0.10	-5.27	-8.41	
[C_4mim][Cl] (p3)	1.95	-4.89	0.36	-5.55	-8.13	7.52
[C_4mim][Cl] (p4)	4.64	-6.17	1.13	-6.29	-6.68	
Mean and Std Dev	2.78 ± 1.43	-5.04 ± 0.83	0.53 ± 0.51	-5.75 ± 0.84	-7.47 ± 0.81	8.60 ± 1.74

Table 2: Differences between SAPT results from two basis sets, E_{SAPT}(aug-cc-pVTZ) − E_{SAPT}(aug-cc-pVDZ). All energies are in kJ·mol^{-1}.

3.0.6 Presentation format

In figure 4 is an example of how the results for each energy are plotted. This is for the Electrostatic energy from the SAPT calculations. The graph is divided into a grid, with the cations on the rows and the anions forming the columns. Methyl imidazolium is "im", and methyl pyrrilidinium is "pyr". For more information about abbreviations used, please refer to table 1. Within the grid, the horizontal axis represents the length of the alkyl

chain on the cation. For example, the induction energy for $[C_1mim][BF_4]$ is plotted in the top left graph as the leftmost point. The different shapes of the points represent the different configurations between the ion pairs. Thus in the previous example the first configuration, called "p1" in the legend, was used. Some ion pairs have more configurations than others. Note that there are missing data points for calculations which have not yet completed successfully. For example, none of the data for $[C_4mim][Ntf_2]$ is available.

3.1 Comparison between methods

Correlation scatterplots have been graphed. These scatterplots are used to convey an idea of how closely the EFP and SAPT numbers agree, and how this is affected by the basis set used and the anion in the system.

These plots have the SAPT energy on the horizontal axis and the EFP energy on the vertical axis. In figure 3

The points are coloured by the anion in the ion pair. The shape indicates the cation. Linear regression has been performed on groups of points where a trend is clearly present. The line $y = x$ is plotted as well to give an idea of how well the two methods agree. The closer the points lie to this line, the better the agreement.

Another way of comparing the two method is by plotting their differences. The differences between each component of the total interaction energy is compared by subtracting the EFP energy from the SAPT energy:

$$E_{\text{abs diff}} = E_{\text{SAPT}} - E_{\text{EFP}}$$

This gives the absolute difference. For the relative error:

$$E_{\text{rel diff}} = \frac{E_{\text{abs diff}}}{E_{\text{SAPT}}}$$

The names for the components differ between the methods. For SAPT, it is electrostatics, exchange, induction, and dispersion that make up the total interaction energy. The SAPT charge-transfer energy is calculated in Psi4 as the difference in total induction between the dimer and mononmer basis sets. This is because in SAPT, the charge-transfer energy is included in the total induction energy, i.e.

$$E_{\text{SAPT}}^{\text{tot Ind}} = E_{\text{SAPT}}^{\text{Ind}} + E_{\text{SAPT}}^{\text{CT}}$$

The components that make up the total EFP interaction energy, in order corresponding to their SAPT equivalents, are electrostatics, repulsion, polarizaton, dispersion, and charge-transfer. In the EFP method, the charge-transfer energy is considered separate from polarization as a part of the total energy.

Therefore, to compare the induction/polarization component between the two methods, the polarization energy will be added to the charge-transfer energy in the EFP method. That is, compare $E_{\text{SAPT}}^{\text{Ind}}$ with $E_{\text{EFP}}^{\text{Pol}} + E_{\text{EFP}}^{\text{CT}}$.

The format for the graphs plotting the difference in energy is very similar to the graphs for the energy plots. Instead of plotting the different configurations, the difference is averaged across the configurations, and the different basis sets used by EFP are compared. There are six plots, one each for electrostatics, exchange-repulsion, induction (polarization), dispersion, charge-transfer and the total interaction energy. These graphs are meant to illustrate how the energy differences across the different ion pairs and basis sets.

Electrostatics Looking at the correlation plots for electrostatics, the agreement between the two methods is clear. The gradient of the trend line is 1.002 with a R^2 value of 0.99.

Considering the plots of the differences, most of the EFP values fall within 25 kJ·mol^{-1}of the SAPT results; only for some instances of the tosylates does EFP overestimate the energy beyond 25 kJ·mol^{-1}. For the imidazoliums, the Pople basis set tends to underestimate the electrostatic energy, whilst the Dunning basis sets overestimate if we exclude the halides. However, for pyrrolidinium systems, in general the triple zeta basis set has the weakest electrostatic interactions (except for NTf_2^-), and is often closer to the SAPT values. cor both cations, often the aug-cc-pVDZ has the largest overestimations; exceptions include the NTf_2^- anion. The EFP results indicate that a basis set of at least up to aug-cc-pVTZ quality is required to treat the tosylate systems well, especially when the system gets larger.

The relative difference in energy across the three basis sets showed the error to be within 5%, except for the tosylates and some halides. In terms of relative error, the electrostatic energy is the best treated out of all the components of the interaction energy. It is crucial that electrostatics is treated well, since this is typically the largest component in the interaction energy.

Looking at the correlation scatterplot, the trend linse follow the centre diagonal fairly closely. The anions with lower electrostatic energies, i.e. towards the top right, show better agreement; it is the halides and the tosylates that deviate more at the higher energies.

Exchange-Repulsion The correlation plots show clear separation between different anions and cations. The halides in the upper right fall closer to the diagonal line,

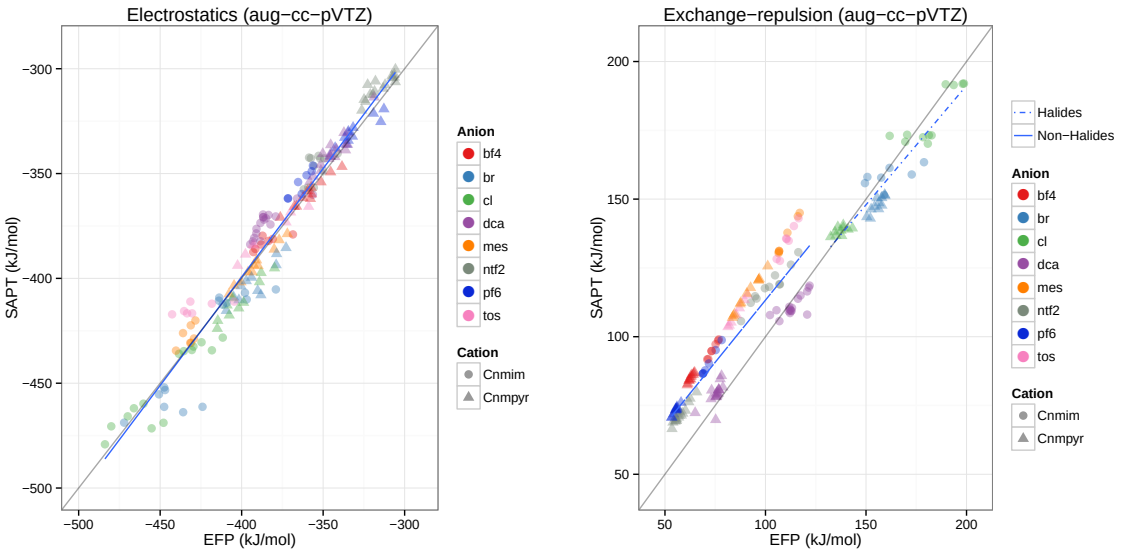

(a) Electrostatics

(b) Exchange-Repulsion

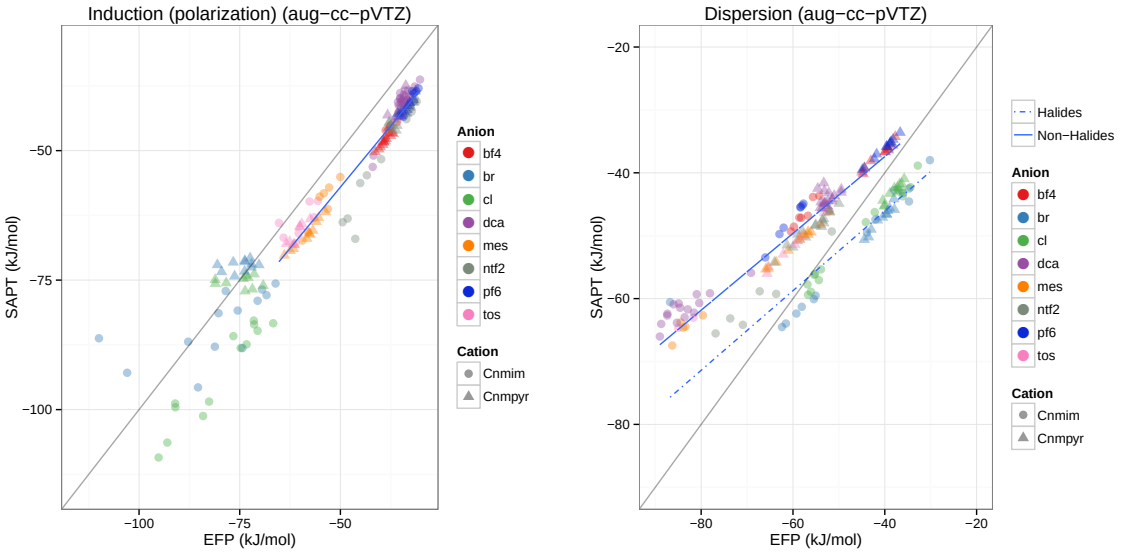

(c) Induction (polarization)

(d) Dispersion

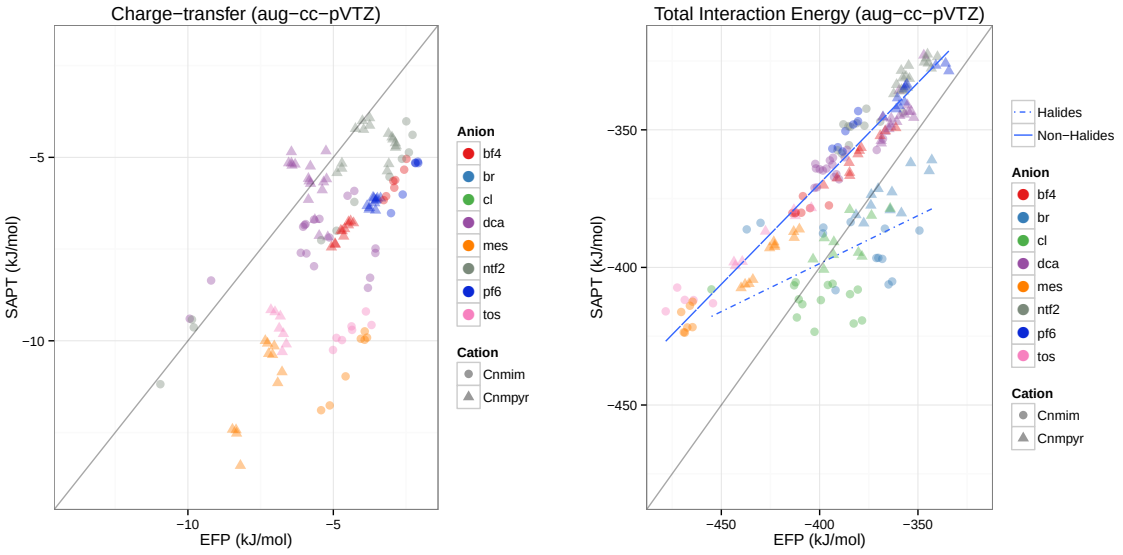

(e) Charge-transfer

(f) Total Interaction Energy

Figure 3: Correlation plots of SAPT and EFP

with a gradient of 1.018 and $R^2 = 0.99$. The non-halide line has a gradient

Here the separation of the different basis sets is clearly seen. As expected, the Dunning basis sets perform much better than the Pople basis set. However, excluding the halides and dicyanamide, surprisingly the triple zeta is worse than the double zeta basis set. In general, the exchange-repulsion interaction is underestimated by the EFP method. This can clearly be seen in the correlation scatterplot, figure 3. The scatterplot also shows the very clear separation between anions. Chloride is handled relatively well, considering that both halides have higher exchange energies compared to the rest of the anions; this is likely due to its smaller size. EFP tends to slightly overestimate the repulsion for imidazolium chloride systems in the Pople and triple zeta basis sets, and overestimate it in the double zeta basis set. In pyrrolidinium chloride systems, EFP slightly underestimates for all three basis sets. Bromide systems were well treated in the aug-cc-pVDZ basis set, but when the Pople basis set is used the error is comparable with that of the other anions, in fact it is the highest amongst the pyrrolidinium systems. When using aug-cc-pVTZ basis set though, the repulsion energy for the bromides is overestimated in both imidazolium and pyrrolidinium. After chloride, dicyanamide is the anion with the lowest errors. Here, the triple zeta basis set performs the best, slightly overestimating the energy for $[C_n\text{mim}][\text{Dca}]$ systems, and underestimating it in all other cases. For the rest of the anions (BF_4^- , Mes^- , NTf_2^- , PF_6^- , and Tos^-), the repulsion is underestimated. The double zeta basis set gives the closest results, followed by triple zeta and then lastly the Pople basis set. Excluding the Pople basis set, most errors were under 25 kJ·mol^{-1}, or around 20% relative error. The Pople basis set gave errors up to nearly 50 kJ·mol^{-1}, for example in the case of the imidazolium mesylates. There is a very slight suggestion that the repulsion energy error increases for imidazolium systems as the length of the alkyl chain increases. There is an equally slight but opposite indication for the pyrrolidinium systems. Referring back to the SAPT results, the trend for exchange to increase for longer alkyl chains in imidazolium is observed, whilst this decreases in pyrrolidinium. Comparing with the EFP results, this pattern is also seen, but to a lesser degree. Hence this is also seen in the difference between the two methods.

Induction (Polarization) Note that to compare the SAPT induction and EFP polarization energies, the EFP charge-transfer energy is summed with the EFP polarization energy. This is because the SAPT method calculates the total induction, which includes the charge-transfer energy. Excepting a few cases of the halides (oddly enough, from the triple zeta basis set), the induction energy is consistently underestimated by the EFP method; most of the points in the correlation scatterplot fall above the line $y = x$. The scatterplot once again highlights the separation between anions. Errors are usually within 10 kJ·mol^{-1}; the worst errors come from the halides in the Pople basis set, which go over 30 kJ·mol^{-1}for the imidazolium bromides. In terms of relative error this translates to within 20%, excluding results from the Pople basis. Here again the Pople basis set has the largest deviations from the SAPT numbers. The Dunning basis sets are comparable for the non-halides, except in tosylates where the triple zeta does better. No data is available for the $[C_n\text{mim}][\text{Tos}]$ systems in the 6-311++G** basis set, though it can be surmised from the corresponding pyrrolidinium systems that they would have larger errors than the Dunning basis sets. Furthermore none of the $[C_n\text{mim}][Ntf_2]$ nor $[C_n\text{mpyr}][Ntf_2]$ results are available since the SAPT results required excessive computational time.

From the SAPT data, the induction energy increases with the length of the alkyl chain on the cation. This trend is reflected in the EFP data as well; for the tetrafluoroborates, the mesylates, hexafluorophosphates and to a lesser extent the dicyanamides and NTf_2^- , though the latter two show less constancy in the energy difference between the two methods. This is more clearly seen in the plots of the relative error, with the error being larger for smaller for the bulkier cations.

The scatterplot also shows how the basis sets agree much better for the anions that have lower energies. The three basis sets diverge when it comes to the more strongly binding anions such as the halides. Surprisingly however, it is the trend line from the Pople basis set that follows the centre diagonal the closest with these more problematic anions; the other two basis sets underestimate considerably. Nevertheless, while the mean of the results may agree better, the deviations within are just as large for the Pople basis as for the Dunning basis.

Dispersion If the halides are excluded, the dispersion energy is usually overestimated, except for BF_4^- and PF_6^- when using the Pople basis set. The halides on the other hand, usually have their dispersion underestimated. Looking at the correlation scatterplot, once again the clustering of the anions is observed. The Pople basis set in many cases gives results closer to the SAPT values than the other two basis sets. This is surprising, as one would expect the Dunning basis sets to have allow a better treatement of dispersion. Again excluding the halides, the absolute difference between SAPT and EFP for dispersion is usually within 10 kJ·mol^{-1}for pyrrolidinium, and within 25 kJ·mol^{-1}for imidazolium. In terms of relative energy, this means within 20% for pyrrolidinium and 40% for imidazolium. The halides have much

larger errors, due to the Pople basis set. If the Pople basis set is not considered, than the halides have error ranges comparable with the other anions. The SAPT results indicate that the dispersion interaction in general increases for bulkier cations, and this trend is well reflected in the EFP results, as there is only slight variation across the different alkyl chain lengths in the errors.

Charge-transfer The absolute error for charge-transfer is small compared to the other interactions (within 10 $kJ{\cdot}mol^{-1}$excluding halides), but the relative error is the highest out of all the components, with most of the pyrrolidinium results above 25% and imidazolium results above 50%. On an absolute scale this difference is not significant, but the relative error makes it obvious. Considering the correlation plot, it is obvious that this is the component with the worst agreement between the two methods. While the halides have much larger absolute errors, they also experience stronger charge-transfer interactions, so their relative errors are comparable with the rest of the anions. However, this means the halides dominate the scatterplot; if they are excluded, then the other anions show better agreement in pattern. The EFP method generally underestimates charge-transfer when compared with SAPT. Charge-transfer was best treated with the aug-cc-pVTZ basis set in every case. In fact, with the triple zeta basis set, the error decreases with increasing alkyl chain length, while it increases for the other two basis sets.

Total interaction energy Interestingly, the halides have the lowest error in the total interaction energy if the Pople basis set is disregarded. This is likely due to the errors from exchange being lower for the halides. The electrostatic energy is usually the most dominant interaction, and the exchange-repulsion cancels this energy out. For imidazolium halides, the tendency is to underestimate the total interaction energy, especially when using the Pople basis set. In the double zeta basis set, the pyrrolidinium bromides have a couple of systems overestimated, while all the pyrrolidinium chloride systems in this basis are overestimated. The rest of the pyrrolidinium halides are underestimated, with the triple zeta basis giving the closest results overall.

The next two anions with the lowest errors are Dca^- and BF_4^- . If the Pople set is excluded, then PF_6^- would belong to this group as well. Here, surprisingly, the Pople basis set seems to have the lowest errors across the different basis sets. For these three systems, in general the Pople basis set slightly underestimates the electrostatic energy, and underestimates the induction energy. However, it treats dispersion better than the Dunning basis sets. This seems to indicate that the Pople basis set is sufficient for smaller ion pairs, but do not treat ion pairs with halides, or larger anions like mesylate and NTf_2^- as well.

For $[C_nmim][Ntf_2]$, there is very little difference between the two Dunning basis sets, but in $[C_nmpyr][Ntf_2]$ the double zeta basis gives better results.

Lastly the tosylates and the mesylates have the highest errors, especially the tosylates. This is probably because of the larger errors from the electrostatic and dispersion components, which were overestimated, coupled with the fact that the repulsion was underestimated. This is more severe for the imidazolium tosylates. The mesylates show little difference between basis sets, across cations with different alkyl chain lengths.

An interesting trend is seen when looking at the scatterplot—ion pairs with less intermolecular attraction are usually better treated than those with high binding energies. While the agreement between SAPT and EFP is not perfect, the EFP energy is usually higher; this consistency is not seen in the other anions. The energies tend to be more scattered towards the left, as the interaction energy increases; another observation is that certain anions tend to be underestimated, whilst others tend to be overestimated.

To give a sense of how the different components contribute to the total interaction energy, figures 40 and 41 show all the energies on the same plot. In the scatterplot (40), the scales of the different components can be seen. In this plot the colours now refer to different basis sets, and the shapes of the points correspond to the different energies. The grid of bar plots in figure 41 is of the absolute errors. It is meant to convey the magnitudes of the error from each component, and how they sum to give the final difference. The colours correspond to the different energies, and the depth of the colour indicates the basis set. Once again, the Boltzmann distribution was used to average the energies across different configurations.

3.2 Charge-transfer and the geodesic scheme

The charge-transfer energies from SAPT and EFP differ by a significant amount. It is the energy with the highest relative error; however, the contribution of the charge-transfer energy to the total interaction energy is relatively small. To further investigate the extent of the charge-transfer interaction, the geodesic charge allocation scheme from the GAMESS package was utilised. This is a computationally cheap method to fit charges to a molecular system, and is routinely used in molecular dynamics simulations. Using this method generates gives each atom on both the cation and anion a charge. Since the ion pair system is neutral, the sum of the charges on the cation should be equal in magnitude and opposite in sign to the sum of the charges on the anion. If there is no charge-transfer, than the total charge on each ion should be unity. However, this

is not observed. Instead, the sum of the charges on an ion was always less than one in magnitude. Subtracting the charge on an ion from unity then gives the amount of charge-transfer that occurred. The same two Dunning basis sets were used in the geodesic scheme, and both basis sets showed very close agreement, with the largest differences being less than 0.01e, where e is the elementary charge. The results from the two basis sets are plotted in figures 42 and 43.

There is however very little correlation (in fact, negative!) between the charge-transfer calculated using SAPT and the geodesic scheme. The correlation coefficient for the aug-cc-pVDZ basis set is 0.51, while the aug-cc-pVTZ basis set has a coefficient of 0.53. This means that the geodesic scheme and the SAPT charge-transfer are somewhat correlated. Calculating the correlation coefficient for the halides alone gives 0.68, which is an even better correlation. On the other hand, the correlation coefficient of the non-halides is -0.05, very slight negative correlation. This indicates that there is no relationship between the SAPT and geodesic scheme numbers for the non-halides.

A scatterplot summarising the data is in figure 44. As can be seen, there is an inverse relationship for the non-halides. While the halides do show some relationship, different systems tend to form their own clusters, indicating there are chemical differences at play here.

4 Conclusion

The interaction energy from the EFP method was compared with that of the SAPT method. The raw energies were discussed, and the differences between the two methods studied. The mean and standard deviation of the differences between SAPT and EFP for each energy from each basis set is tabulated in tables 3 and 4. For each basis set there are two columns, the first one on the right is the mean, and the second column the standard deviation. There are two tables, on for the halides and the other for the other anions. This is due to the differences between the two groups, especially in the exchange-repulsion and charge-transfer energies.

	Halides					
Energy	aug-cc-pVDZ		aug-cc-pVTZ		6-311++G**	
Electrostatics	13.0	(± 9.5)	-7.95	(± 9.3)	-10.7	(± 10.1)
Exchange-repulsion	1.3	(± 7.2)	-7.01	(± 15.1)	21.1	(± 20.8)
Induction-polarization	-6.4	(± 6.3)	-0.19	(± 11.6)	-25.4	(± 6.8)
Dispersion	-9.3	(± 1.6)	-4.46	(± 4.9)	-26.0	(± 3.6)
Charge-transfer	-34.3	(± 14.4)	-24.72	(± 18.5)	-29.6	(± 15.4)
Total Energy	-1.3	(± 18.9)	-9.79	(± 23.0)	-36.3	(± 21.3)

Table 3: Summary statistics for halides

It seems that for the halides, the charge-transfer energy contributes much to the error; this is followed by the repulsion and polarization components. The aug-cc-pVTZ basis set handles the halides best overall, particularly if the charge-transfer is not considered. For the other anions, the component with the largest error overall is repulsion. This can be clearly seen for the tetrafluoroborates, the hexafluorophosphates, the mesylates and also NTf_2^-. In the tosylates, the Coulomb interaction also contributes significantly to the difference. The induction term is typically underestimated, while the dispersion term is overestimated consistently, indicating a systematic difference between SAPT and EFP for these two terms. This results in some cancelling because these two energies are of a somewhat similar scale (typical magnitude around 10 kJ·mol^{-1} usually below 20 kJ·mol^{-1}) in the systems studied. Furthermore, using the Fock matrix alone to calculate the exchange-repulsion gives large errors; this is another aspect of the EFP method that can be improved. Figure 40 provides a nice summary of the differences. It puts into perspective the different scales of the different components. Exchange-repulsion is consistently underestimated in the upper right, induction and dispersion terms fall on opposite sides of the diagonal line at energies between -100 and 0 kJ·mol^{-1}, while the charge-transfer data sits close to zero, showing how for most cases it has but a tiny contribution. The electrostatic component along with the total interaction energy populate the lower left. Their proximity to one another shows that the Coulomb interaction dominates, which is expected for charged species.

Acknowledgements

We gratefully acknowledge computer grants from the Monash eResearch Centre, MASSIVE and the National Computational Infrastructure. This work is supported by the ARC - DP Grant and a Future Fellowship for EII.

References

[1] K. Wendler et al. "Ionic liquids studied across different scales: A computational perspective". In: *Faraday Discussions* 154

Non-halides						
Energy	aug–cc-pVDZ		aug-cc-pVTZ		6-311++G**	
Electrostatics	9.0	(± 11.1)	4.6	(± 6.5)	3.4	(± 9.3)
Exchange-repulsion	13.6	(± 6.3)	14.8	(± 9.4)	30.0	(± 11.3)
Induction-polarization	-6.3	(± 2.2)	-5.7	(± 2.2)	-9.7	(± 2.3)
Dispersion	10.5	(± 6.9)	11.1	(± 6.7)	2.0	(± 5.6)
Charge-transfer	-5.3	(± 1.8)	-2.3	(± 1.9)	-3.9	(± 1.5)
Total Energy	26.9	(± 15.0)	27.8	(±12.4)	27.0	(± 16.1)

Table 4: Summary statistics for non-halides

(2012), p. 111. ISSN: 1359-6640, 1364-5498. DOI: 10.1039/c1fd00051a. URL: http://xlink.rsc.org/?DOI=c1fd00051a (visited on 07/23/2013).

[2] D. Bedrov et al. "Influence of Polarization on Structural, Thermodynamic, and Dynamic Properties of Ionic Liquids Obtained from Molecular Dynamics Simulations". In: *The Journal of Physical Chemistry B* 114.15 (Apr. 2010), pp. 4984–4997. ISSN: 1520-6106, 1520-5207. DOI: 10.1021/jp911670f. URL: http://pubs.acs.org/doi/abs/10.1021/jp911670f (visited on 07/23/2013).

[3] E. I. Izgorodina. "Towards large-scale, fully ab initio calculations of ionic liquids". In: *Physical Chemistry Chemical Physics* 13.10 (2011), p. 4189. ISSN: 1463-9076, 1463-9084. DOI: 10.1039/c0cp02315a. URL: http://xlink.rsc.org/?DOI=c0cp02315a (visited on 07/23/2013).

[4] A. J. Stone. *The theory of intermolecular forces*. English. International Series of Monographs on Chemistry. Oxford; Oxford; New York: Clarendon Press ; Oxford University Press, 1996. ISBN: 019855883X 9780198558835 0198558848 9780198558842. URL: http://books.google.com.au/books?id=nQvhXDVnmowC.

[5] J. M. Turney et al. "Psi4: an open-source *ab initio* electronic structure program". In: *Wiley Interdisciplinary Reviews: Computational Molecular Science* 2.4 (July 2012), pp. 556–565. ISSN: 17590876. DOI: 10.1002/wcms.93. URL: http://doi.wiley.com/10.1002/wcms.93 (visited on 07/23/2013).

[6] J. H. Jensen and M. S. Gordon. "An approximate formula for the intermolecular Pauli repulsion between closed shell molecules. II. Application to the effective fragment potential method". In: *The Journal of Chemical Physics* 108.12 (1998), p. 4772. ISSN: 00219606. DOI: 10.1063/1.475888. URL: http://link.aip.org/link/JCPSA6/v108/i12/p4772/s1&Agg=doi (visited on 07/25/2013).

[7] M. S. Gordon et al. "The Effective Fragment Potential Method: A QM-Based MM Approach to Modeling Environmental Effects in Chemistry". In: *The Journal of Physical Chemistry A* 105.2 (Jan. 2001), pp. 293–307. ISSN: 1089-5639, 1520-5215. DOI: 10.1021/jp002747h. URL: http://pubs.acs.org/doi/abs/10.1021/jp002747h (visited on 07/23/2013).

[8] M. S. Gordon et al. "Accurate Methods for Large Molecular Systems ". In: *The Journal of Physical Chemistry B* 113.29 (July 2009), pp. 9646–9663. ISSN: 1520-6106, 1520-5207. DOI: 10.1021/jp811519x. URL: http://pubs.acs.org/doi/abs/10.1021/jp811519x (visited on 07/23/2013).

[9] J. M. Mullin et al. "Systematic Fragmentation Method and the Effective Fragment Potential: An Efficient Method for Capturing Molecular Energies". In: *The Journal of Physical Chemistry A* 113.37 (Sept. 2009), pp. 10040–10049. ISSN: 1089-5639, 1520-5215. DOI: 10.1021/jp9036183. URL: http://pubs.acs.org/doi/abs/10.1021/jp9036183 (visited on 07/23/2013).

[10] M. S. Gordon et al. "Fragmentation Methods: A Route to Accurate Calculations on Large Systems". In: *Chemical Reviews* 112.1 (Jan. 2012), pp. 632–672. ISSN: 0009-2665, 1520-6890. DOI: 10.1021/cr200093j. URL: http://pubs.acs.org/doi/abs/10.1021/cr200093j (visited on 07/23/2013).

[11] P. N. Day et al. "An effective fragment method for modeling solvent effects in quantum mechanical calculations". In: *The Journal of Chemical Physics* 105.5 (1996), p. 1968. ISSN: 00219606. DOI: 10.1063/1.472045. URL: http://link.aip.org/link/JCPSA6/v105/i5/p1968/s1&Agg=doi (visited on 07/23/2013).

[12] W. Chen and M. S. Gordon. "Energy decomposition analyses for many-body interaction and applications to water complexes". In: *The Journal of Physical Chemistry* 100.34 (1996), pp. 14316–14328. URL: http://pubs.acs.org/doi/abs/10.1021/jp960694r (visited on 07/23/2013).

[13] I. Adamovic and M. S. Gordon. "MethanolWater Mixtures: A Microsolvation Study Using the Effective Fragment Potential Method". In: *The Journal of Physical Chemistry A* 110.34 (Aug. 2006), pp. 10267–10273. ISSN: 1089-5639, 1520-5215. DOI: 10.1021/jp060607n. URL: http://pubs.acs.org/doi/abs/10.1021/jp060607n (visited on 07/23/2013).

[14] M. S. Gordon et al. "Chapter 10 The Effective Fragment Potential: A General Method for Predicting Intermolecular Interactions". en. In: *Annual Reports in Computational Chemistry*. Vol. 3. Elsevier, 2007, pp. 177–193. ISBN: 9780444530882. URL: http://linkinghub.elsevier.com/retrieve/pii/S1574140007030101 (visited on 03/14/2014).

[15] D. Ghosh et al. "Noncovalent Interactions in Extended Systems Described by the Effective Fragment Potential Method: Theory and Application to Nucleobase Oligomers". In: *The Journal of Physical Chemistry A* 114.48 (Dec. 2010), pp. 12739–12754. ISSN: 1089-5639, 1520-5215. DOI: 10.1021/jp107557p. URL: http://pubs.acs.org/doi/abs/10.1021/jp107557p (visited on 07/23/2013).

[16] J. C. Flick et al. "Accurate Prediction of Noncovalent Interaction Energies with the Effective Fragment Potential Method: Comparison of Energy Components to Symmetry-Adapted Perturbation Theory for the S22 Test Set". In: *Journal of Chemical Theory and Computation* 8.8 (Aug. 2012), pp. 2835–2843. ISSN: 1549-9618, 1549-9626. DOI: 10.1021/ct200673a. URL: http://pubs.acs.org/doi/abs/10.1021/ct200673a (visited on 07/23/2013).

[17] P. Jureka et al. "Benchmark database of accurate (MP2 and CCSD(T) complete basis set limit) interaction energies of small model complexes, DNA base pairs, and amino acid pairs". en. In: *Physical Chemistry Chemical Physics* 8.17 (Apr. 2006), pp. 1985–1993. ISSN: 1463-9084. DOI: 10.1039/B600027D. URL: http://pubs.rsc.org/en/content/articlelanding/2006/cp/b600027d (visited on 03/18/2014).

[18] J. ezá, K. E. Riley, and P. Hobza. "S66: A Well-balanced Database of Benchmark Interaction Energies Relevant to Biomolecular Structures". In: *Journal of Chemical Theory and Computation* 7.8 (Aug. 2011), pp. 2427–2438. ISSN: 1549-9618. DOI: 10.1021/ct2002946. URL: http://dx.doi.org/10.1021/ct2002946 (visited on 03/31/2014).

[19] R. Eisenschitz and F. London. "ber das Verhltnis der van der Waalsschen Krfte zu den homopolaren Bindungskrften". In: *Zeitschrift fr Physik* 60.7-8 (July 1930), pp. 491–527. ISSN: 1434-6001, 1434-601X. DOI: 10.1007/BF01341258. URL: http://link.springer.com/10.1007/BF01341258 (visited on 07/23/2013).

[20] B. Jeziorski, R. Moszynski, and K. Szalewicz. "Perturbation theory approach to intermolecular potential energy surfaces of van der Waals complexes". In: *Chemical Reviews* 94.7 (1994), pp. 1887–1930. URL: http://pubs.acs.org/doi/pdf/10.1021/cr00031a008 (visited on 07/23/2013).

[21] E. G. Hohenstein and C. D. Sherrill. "Density fitting and Cholesky decomposition approximations in symmetry-adapted perturbation theory: Implementation and application to probe the nature of - interactions in linear acenes". In: *The Journal of Chemical Physics* 132.18 (May 2010), pp. 184111–184111. ISSN: 00219606. DOI: doi:10.1063/1.3426316. URL: http://jcp.aip.org/resource/1/jcpsa6/v132/i18/p184111_s1 (visited on 07/24/2013).

[22] E. G. Hohenstein and C. D. Sherrill. "Density fitting of intramonomer correlation effects in symmetry-adapted perturbation theory". In: *The Journal of Chemical Physics* 133.1 (July 2010), pp. 014101–014101. ISSN: 00219606. DOI: doi:10.1063/1.3451077. URL: http://jcp.aip.org/resource/1/jcpsa6/v133/i1/p014101_s1 (visited on 07/24/2013).

[23] E. G. Hohenstein and C. D. Sherrill. "Efficient evaluation of triple excitations in symmetry-adapted perturbation theory via second-order MollerPlesset perturbation theory natural orbitals". In: *The Journal of Chemical Physics* 133.10 (2010), p. 104107. ISSN: 00219606. DOI: 10.1063/1.3479400. URL: http://link.aip.org/link/JCPSA6/v133/i10/p104107/s1&Agg=doi (visited on 07/23/2013).

[24] E. G. Hohenstein et al. "Large-scale symmetry-adapted perturbation theory computations via density fitting and Laplace transformation techniques: Investigating the fundamental forces of DNA-intercalator interactions". In: *The Journal of Chemical Physics* 135.17 (2011), p. 174107. ISSN: 00219606. DOI: 10.1063/1.3656681. URL: http://link.aip.org/link/JCPSA6/v135/i17/p174107/s1&Agg=doi (visited on 07/23/2013).

[25] E. G. Hohenstein and C. D. Sherrill. "Wavefunction methods for noncovalent interactions". In: *Wiley Interdisciplinary Reviews: Computational Molecular Science* 2.2 (Mar. 2012), pp. 304–326. ISSN: 17590876. DOI: 10.1002/wcms.84. URL: http://doi.wiley.com/10.1002/wcms.84 (visited on 07/23/2013).

A Figures

Due to the large number of figures, they have been included here as supplementary information. The first section consists of plots of all the raw energies. Figures 4, 5, 6, 7, 8 and 9 are from the SAPT method, using the aug-cc-pVDZ basis set. What follows are the EFP results. Figures 10, 11, 12, 13, 14 and 15 were obtained from the aug-cc-pVDZ basis set as well. Figures 16, 17, 18, 19, 20 and 21 are from the aug-cc-pVTZ basis set.

Lastly, figures 22, 23, 24, 25, 26 and 27 are from the 6-311++G** basis set.

The next set of plots of the differences between SAPT and EFP results. For each energy, there is a plot of the absolute differences followed by a plot of the relative differences. The order of energies follow that of the previous plots, i.e. electrostatics, exchange-repulsion, induction-polarization, dispersion, charge-transfer and then the total interaction energy. These are displayed in figures 28 through to 38 and figure 39.

A final plot that has all of the different energies together is figure 40. This time the shape of a point indicates which energy it is, and the colour corresponds to the basis set.

The geodesic scheme results from the two basis sets used are plotted next, in graphs 42 and 43. The correlation with the charge-transfer energy from SAPT is shown in 44. Note the scales of the axis.

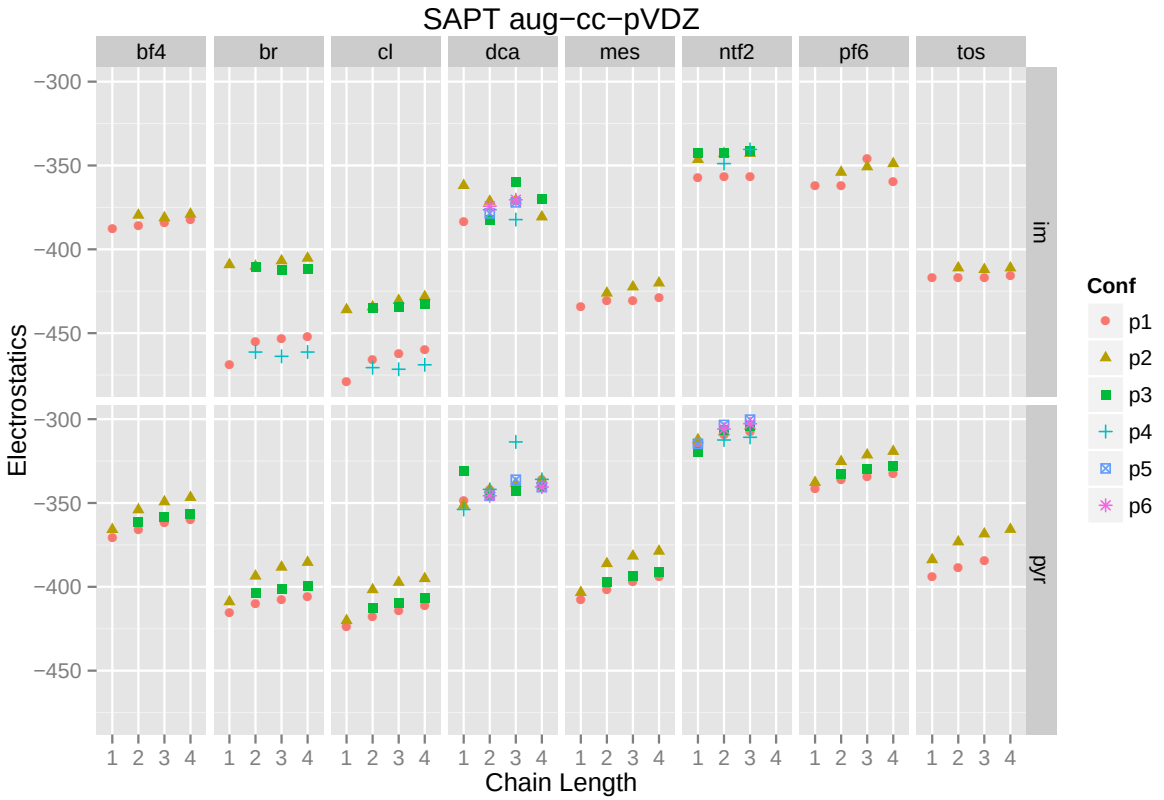

Figure 4: SAPT Electrostatic Energy

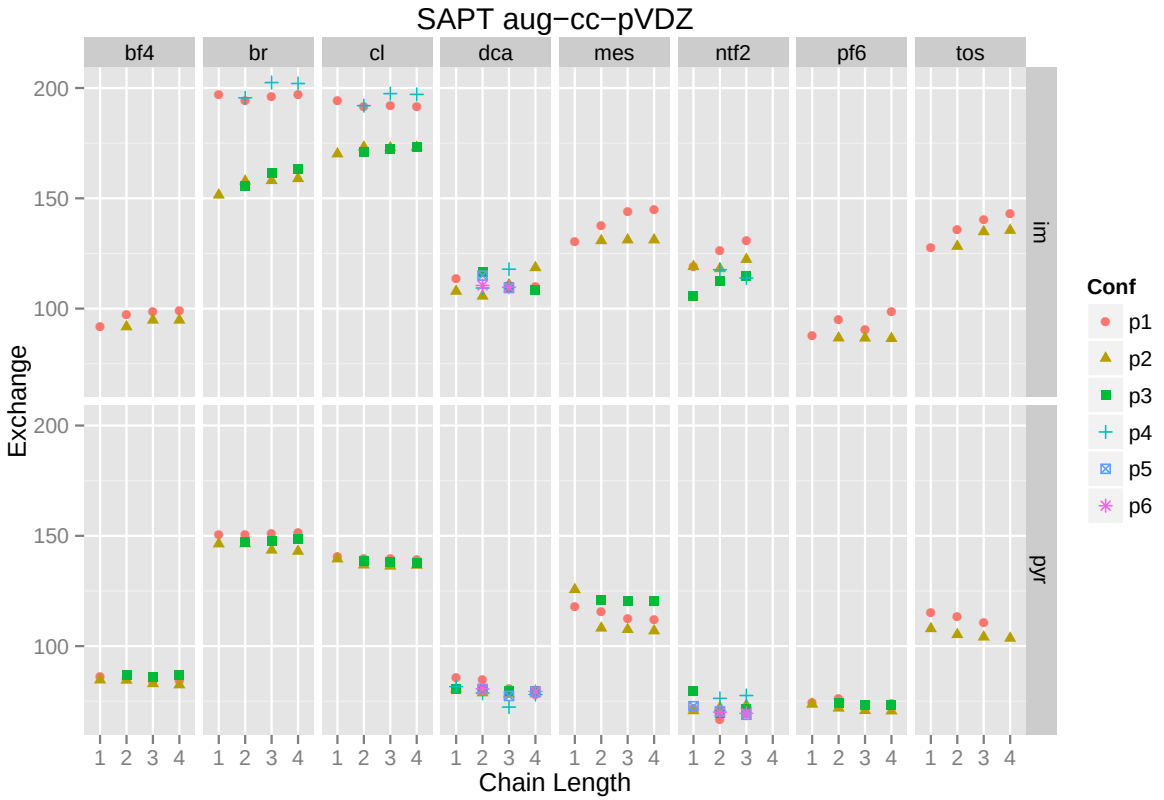

Figure 5: SAPT Exchange Energy

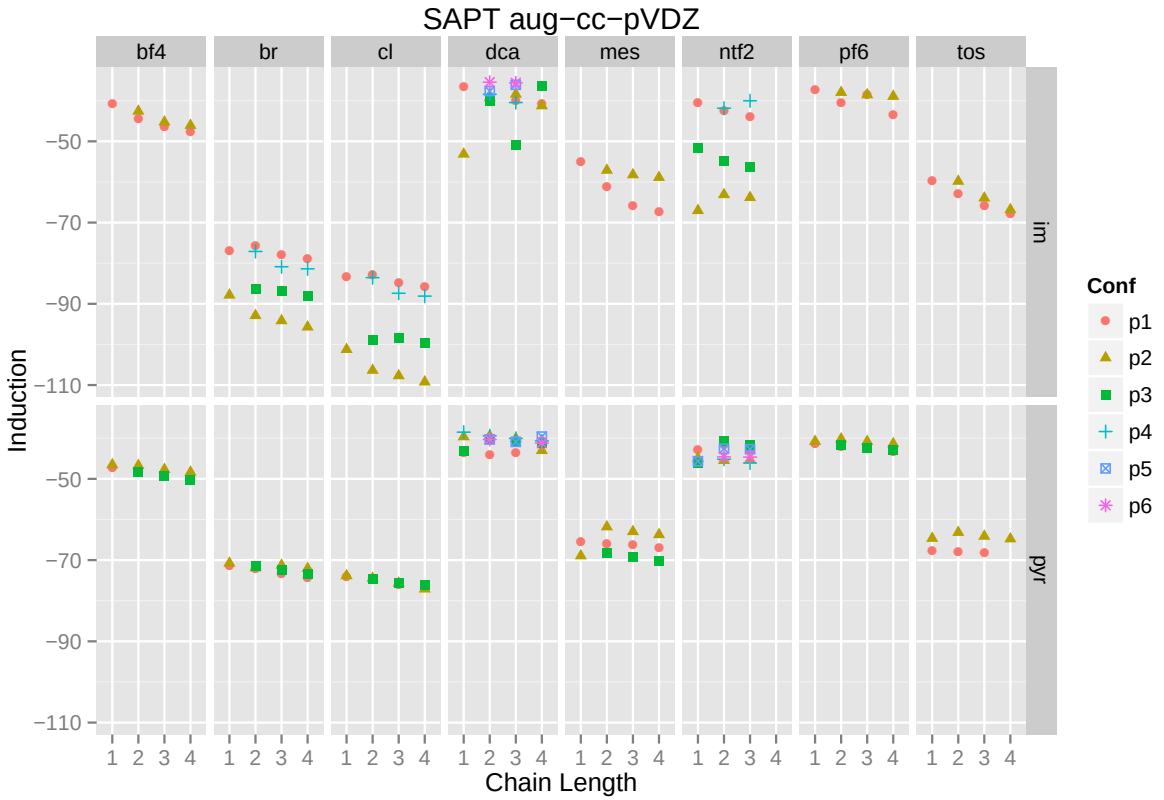

Figure 6: SAPT Induction Energy

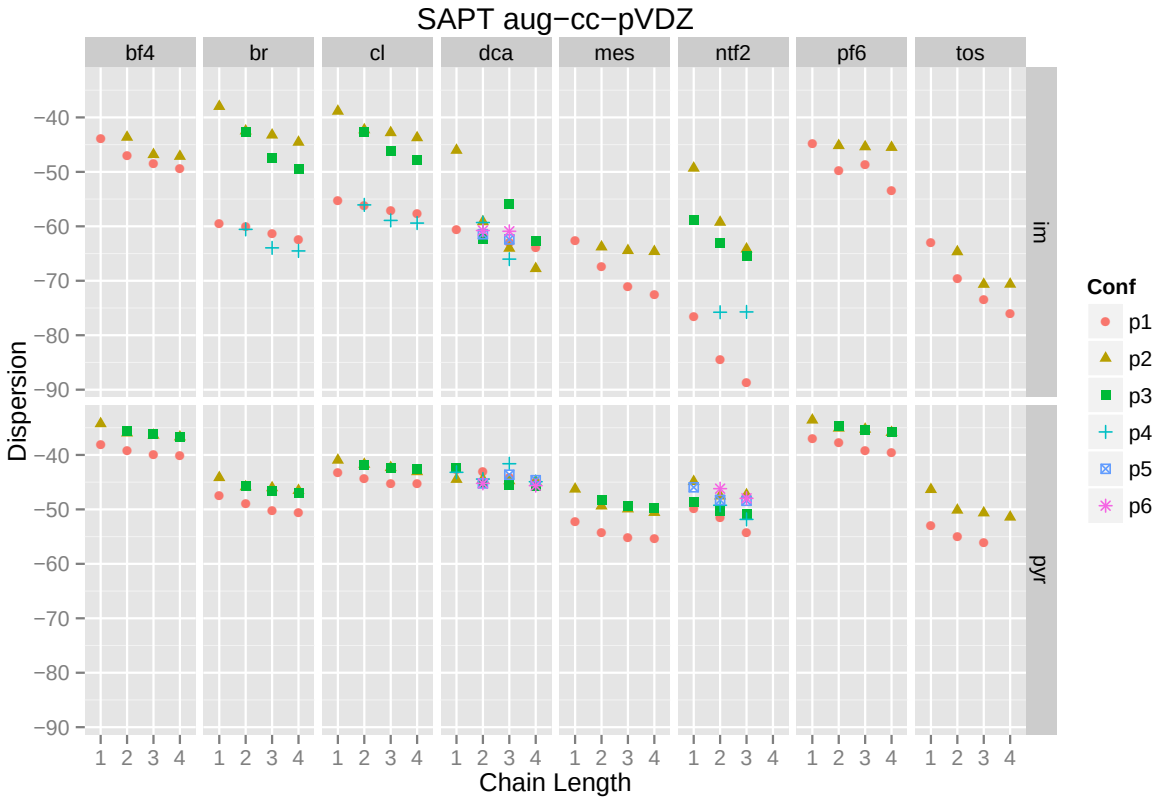

Figure 7: SAPT Dispersion Energy

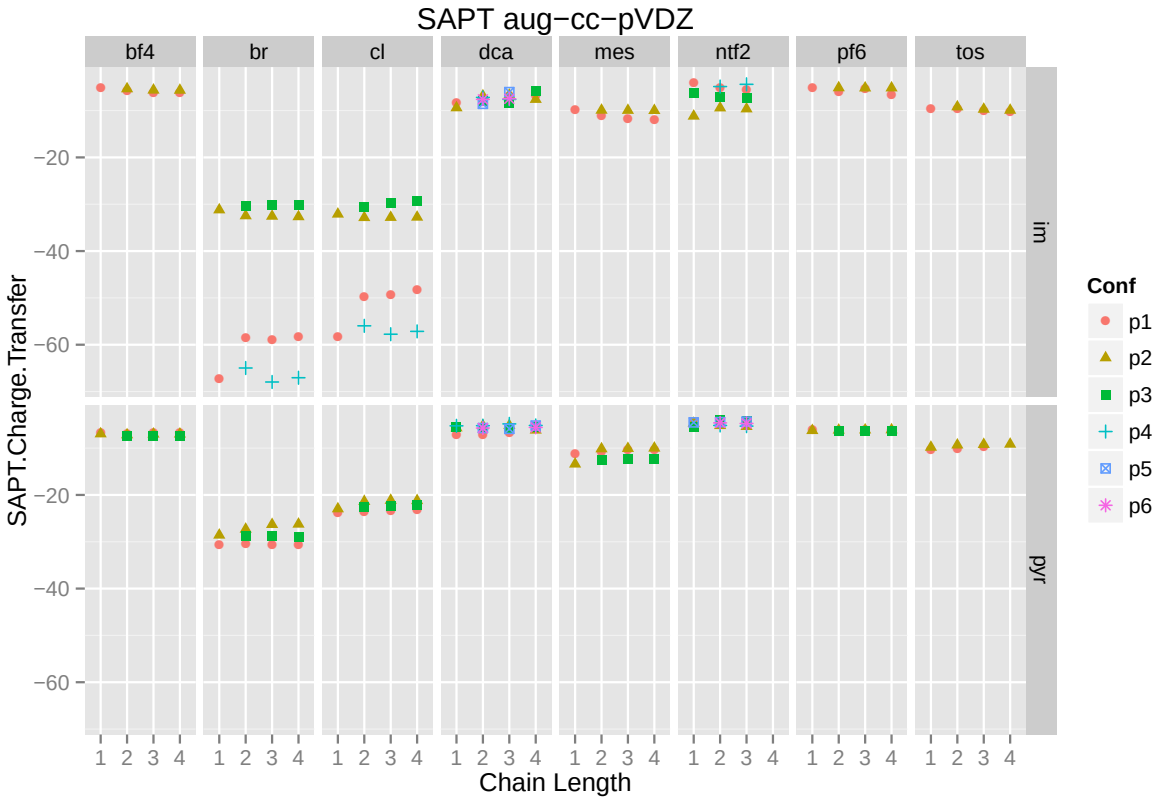

Figure 8: SAPT Charge-transfer Energy

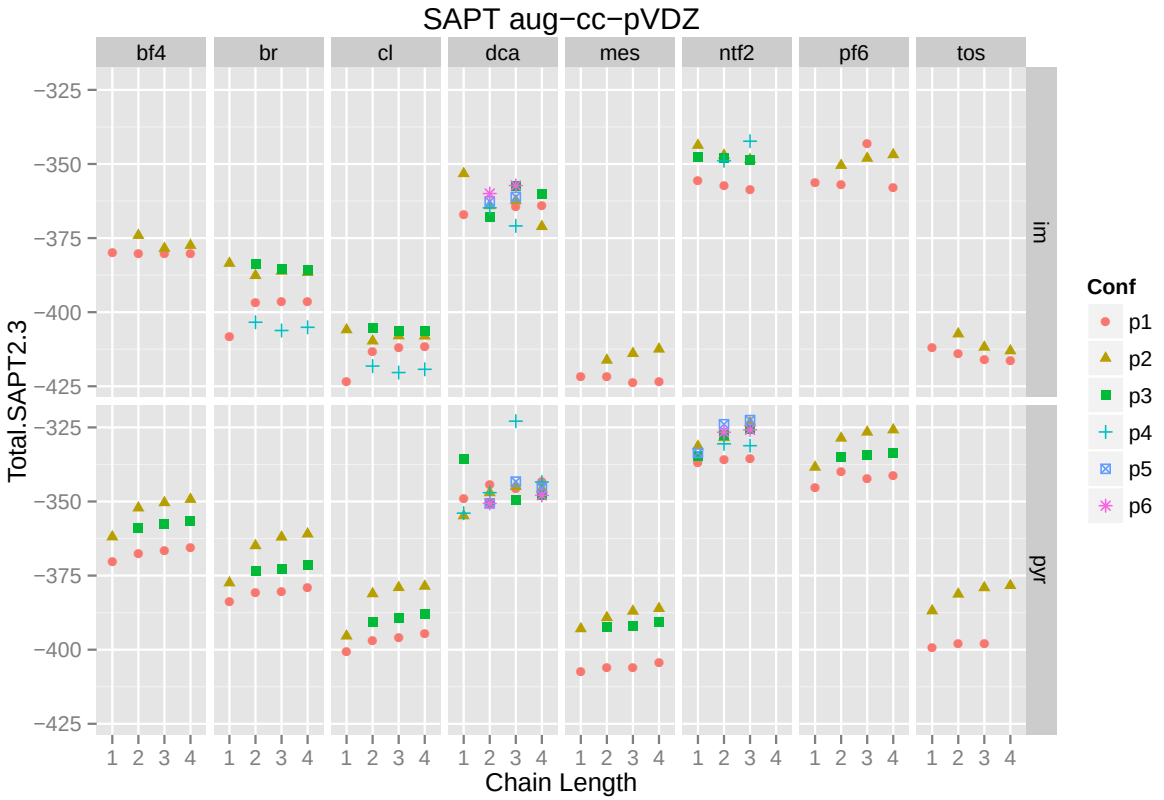

Figure 9: SAPT Total Energy

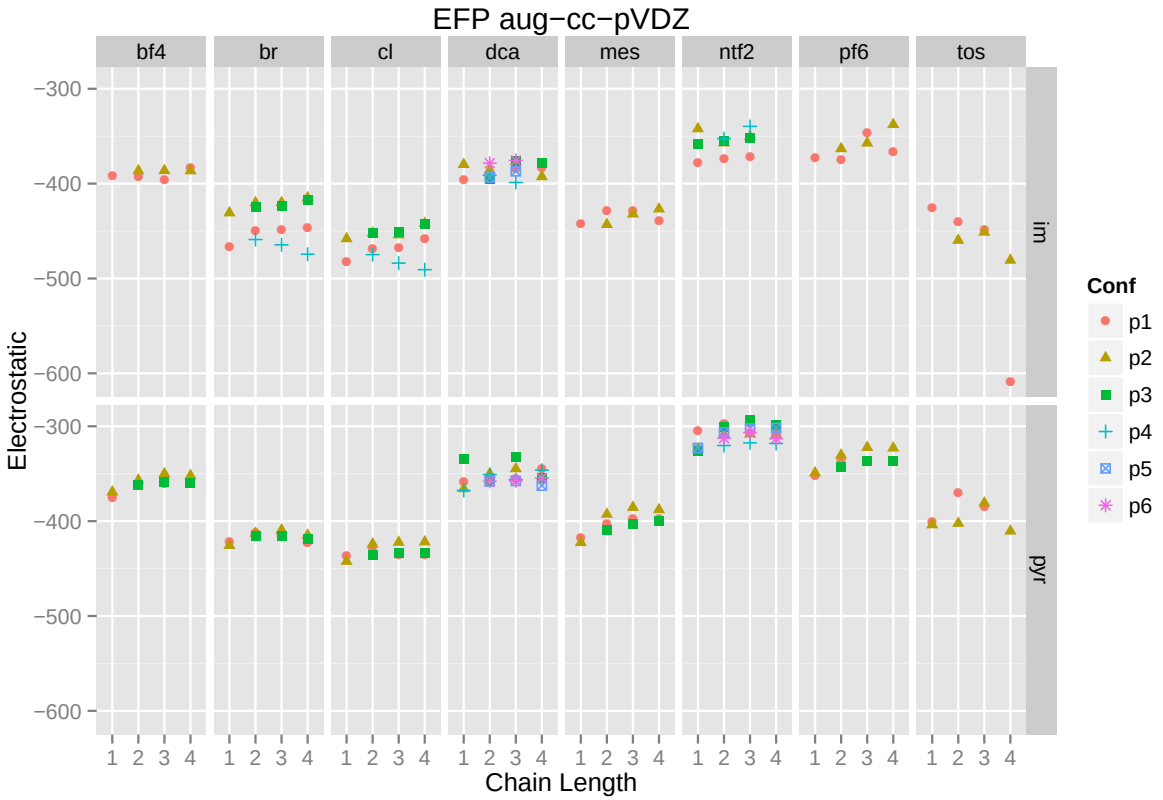

Figure 10: EFP Electrostatic Energy

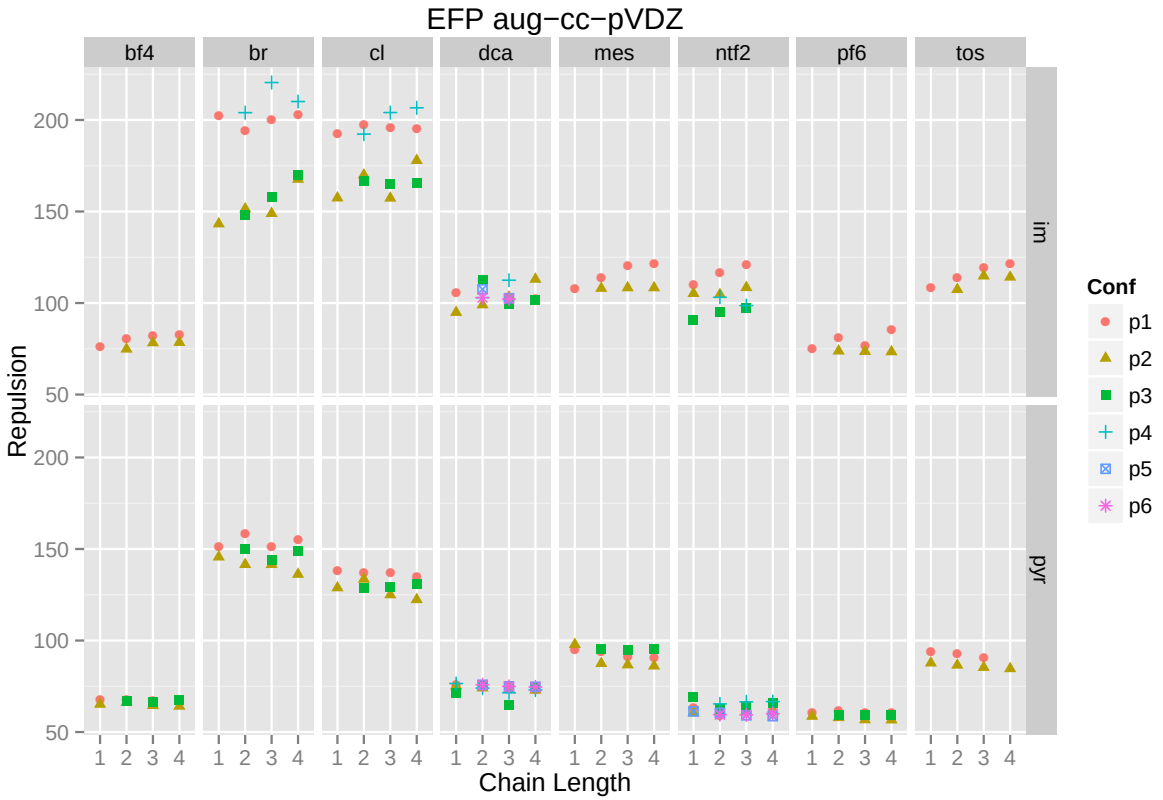

Figure 11: EFP Repulsion Energy

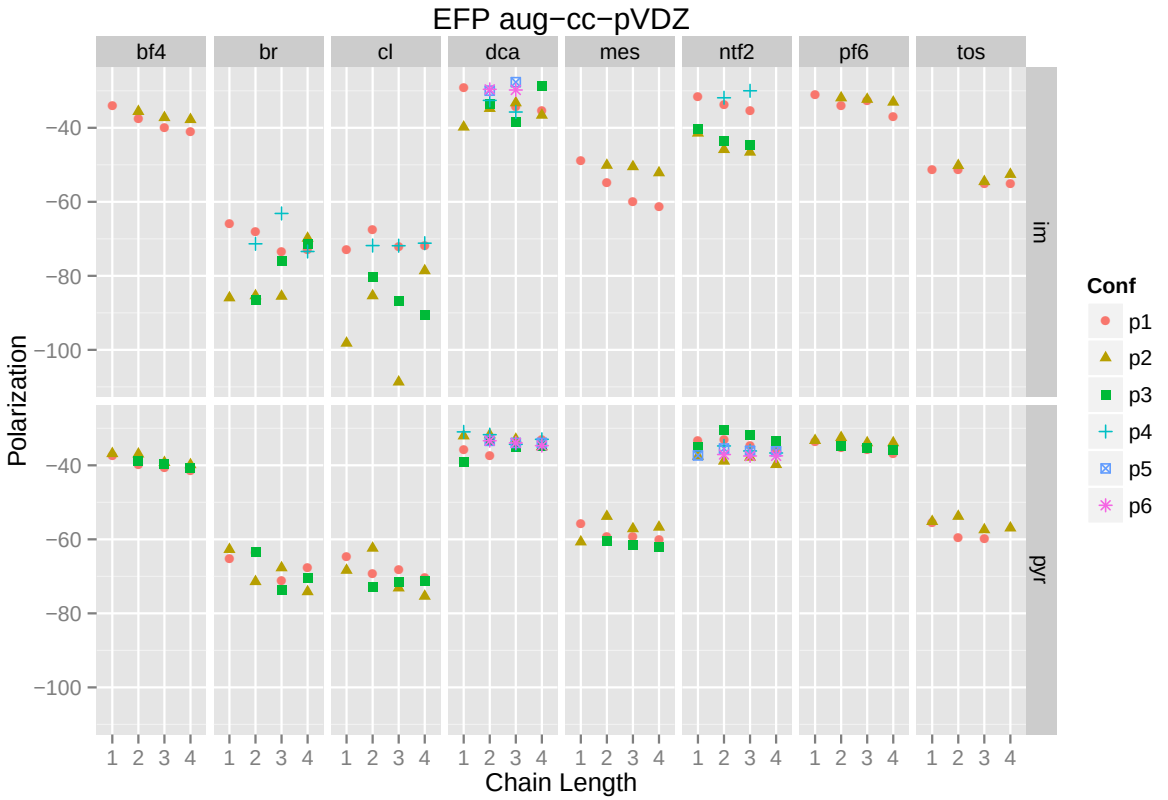

Figure 12: EFP Polarization Energy

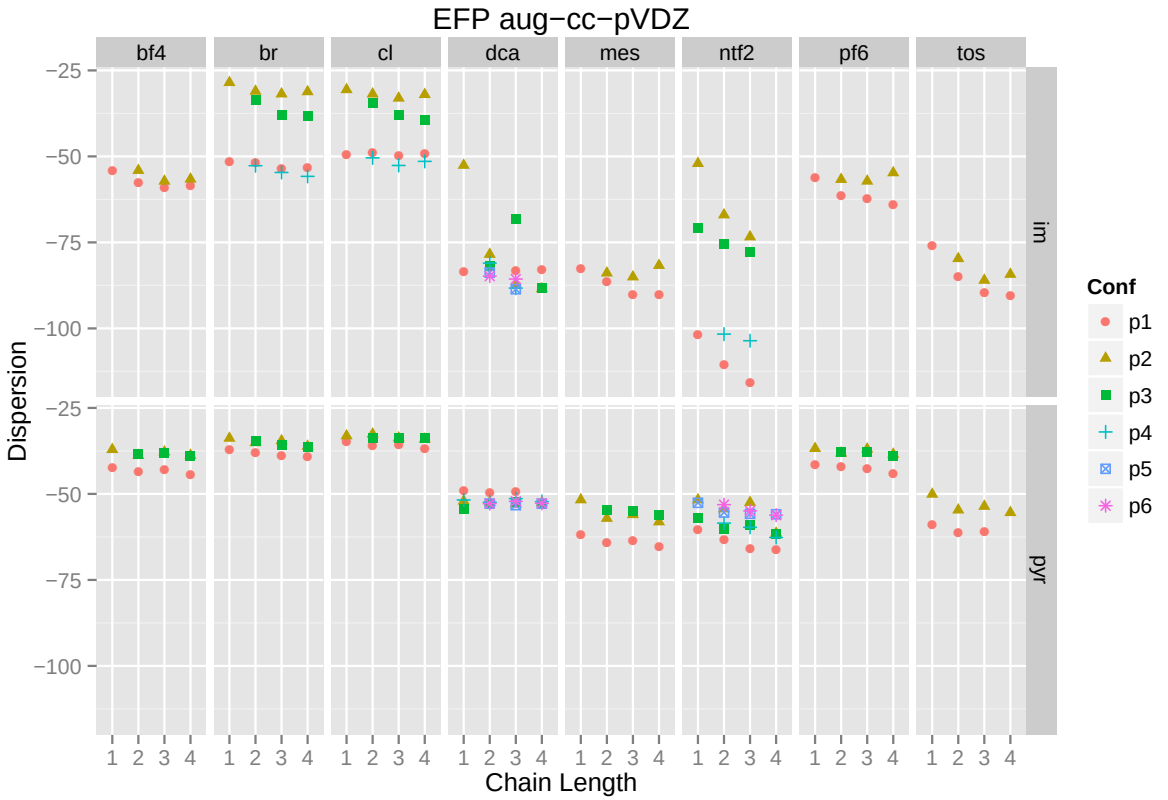

Figure 13: EFP Dispersion Energy

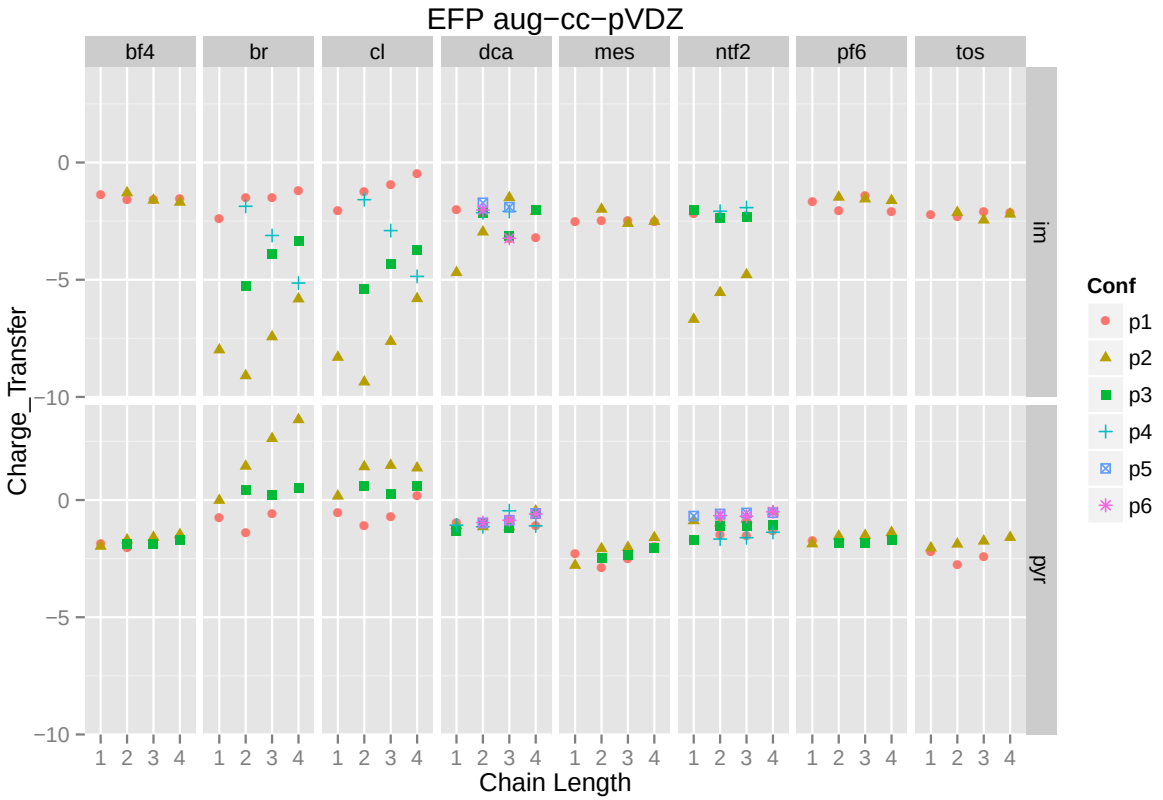

Figure 14: EFP Charge-transfer Energy

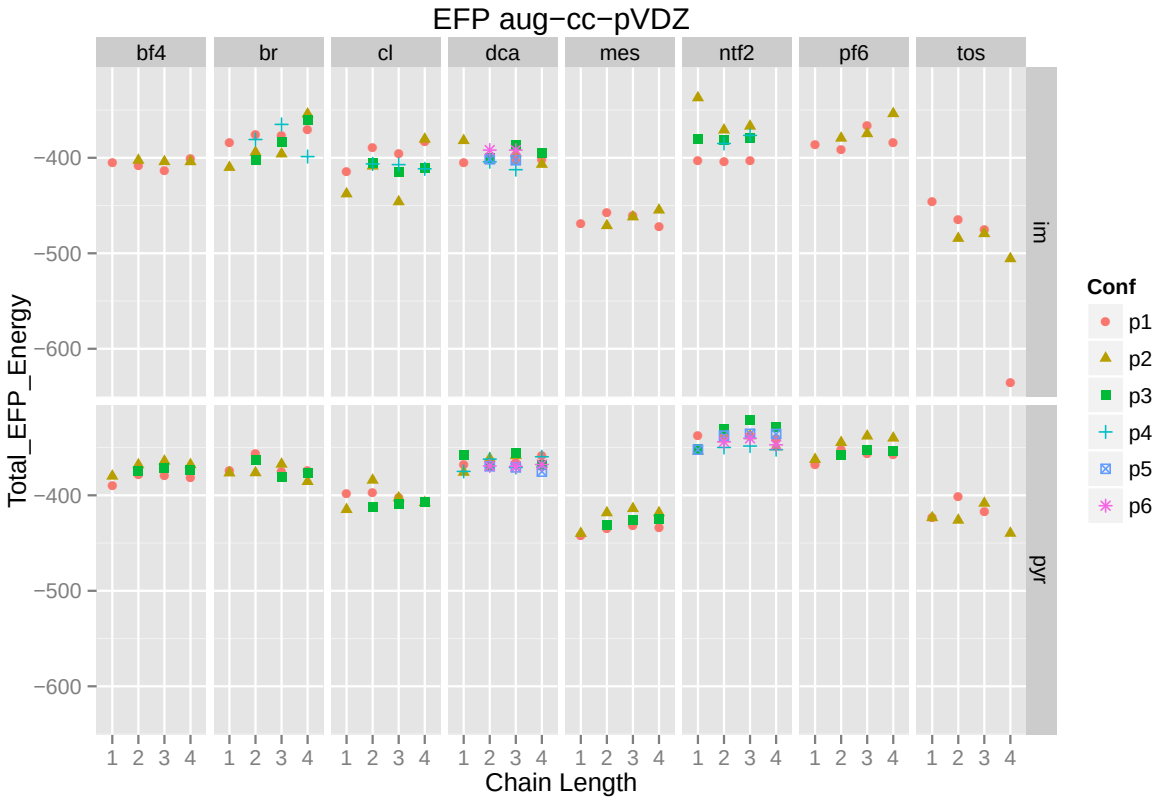

Figure 15: EFP Total Energy

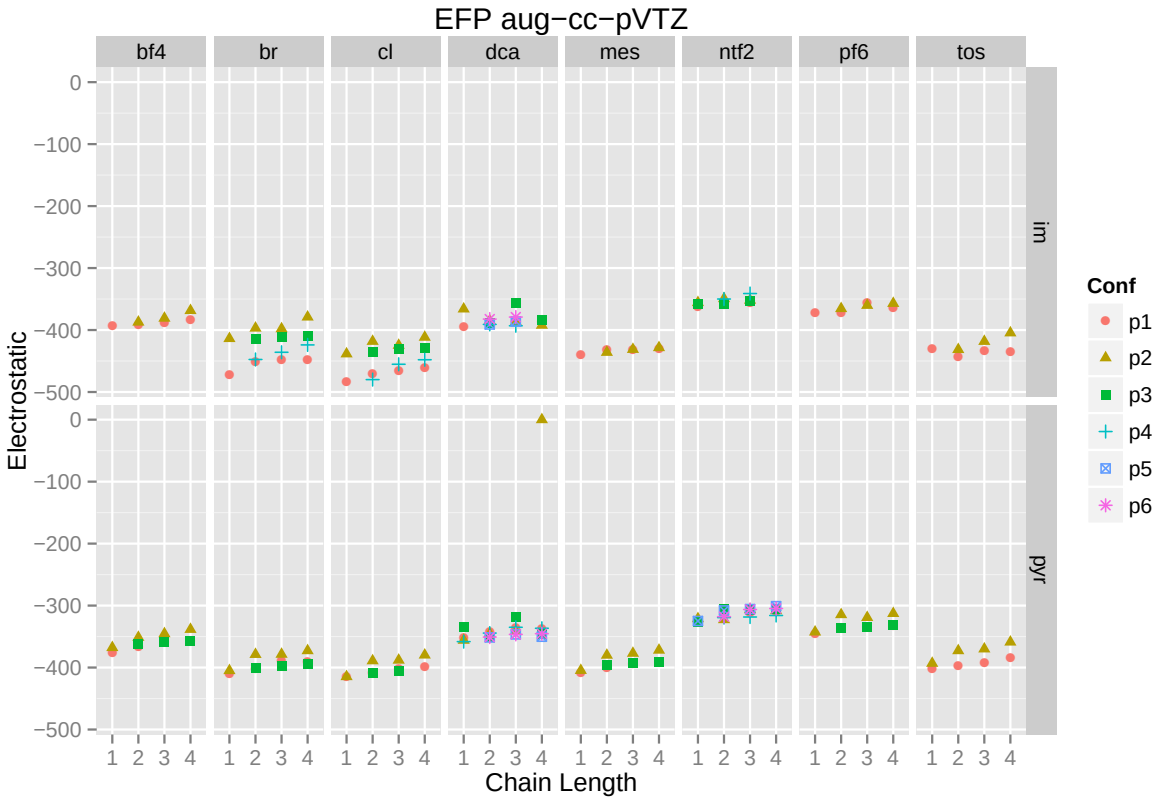

Figure 16: EFP Electrostatic Energy

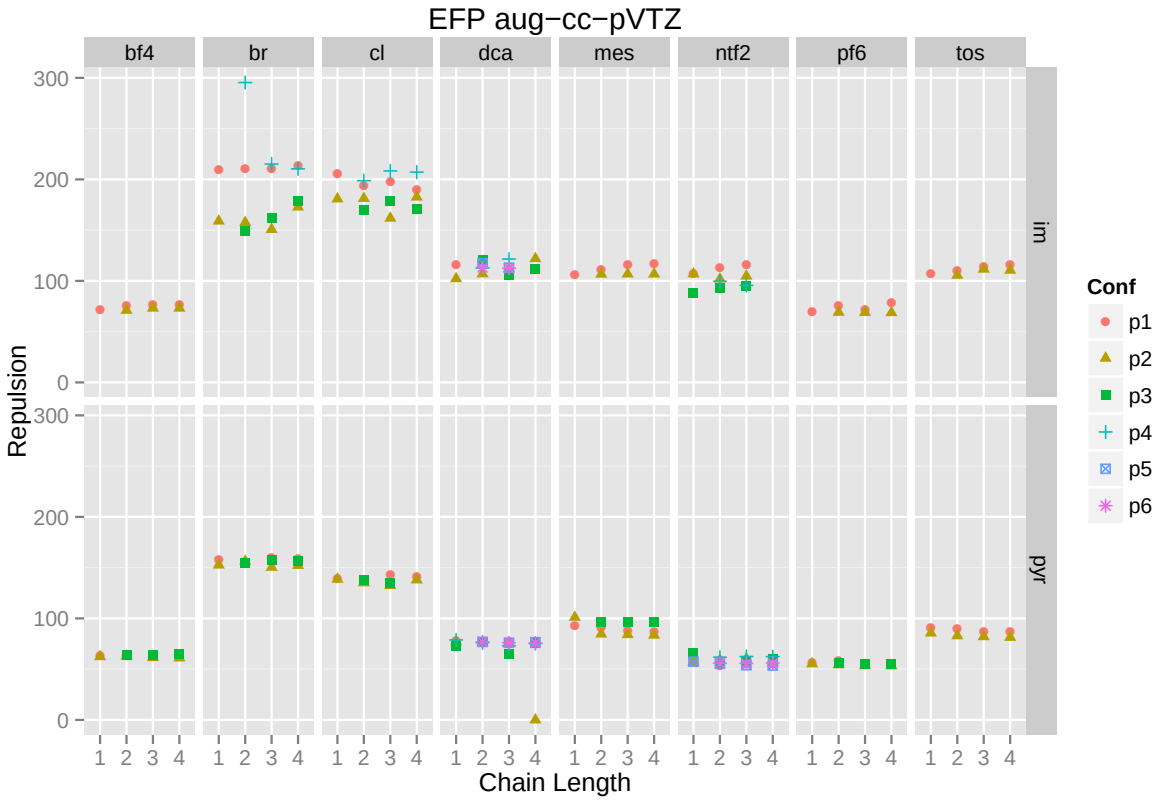

Figure 17: EFP Repulsion Energy

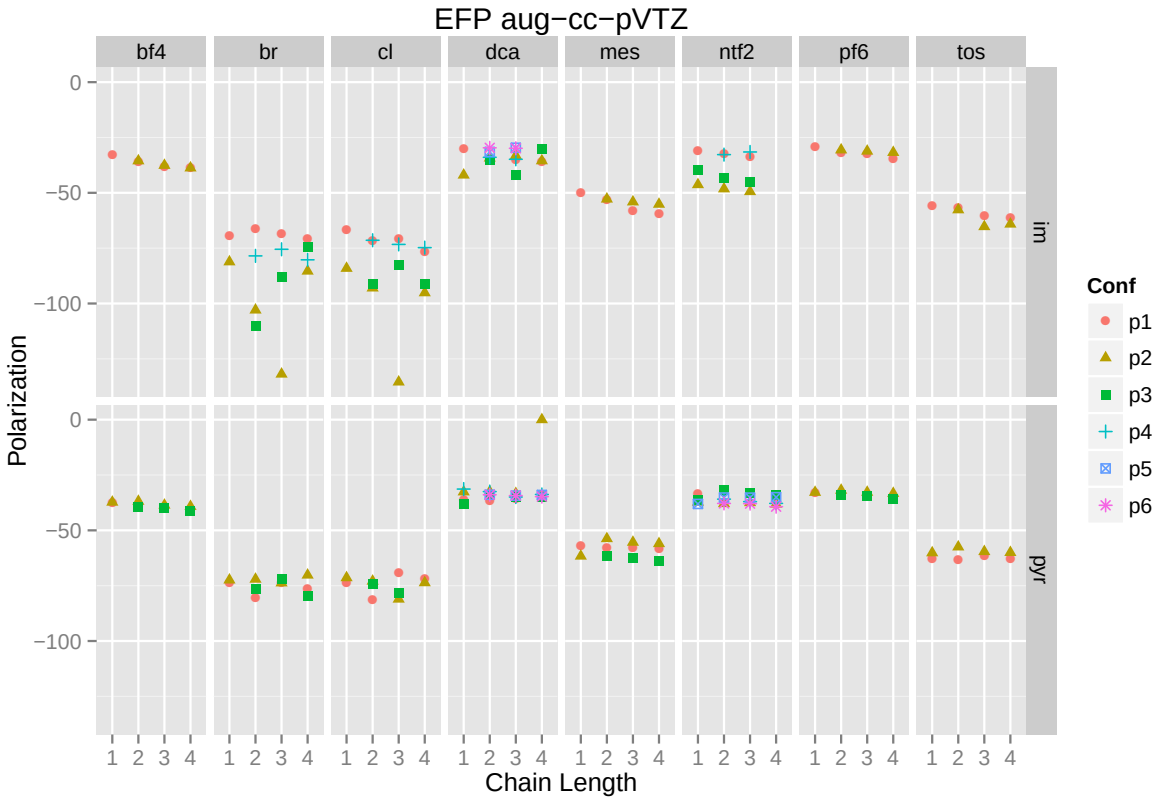

Figure 18: EFP Polarization Energy

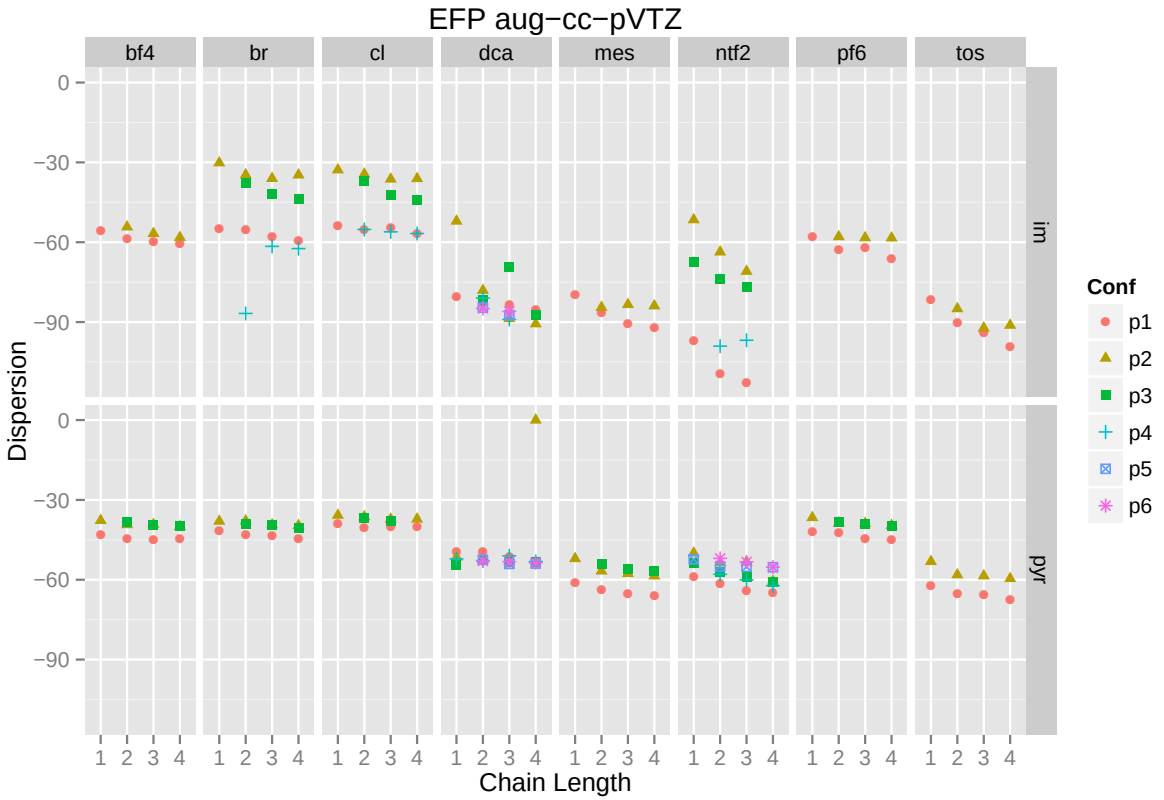

Figure 19: EFP Dispersion Energy

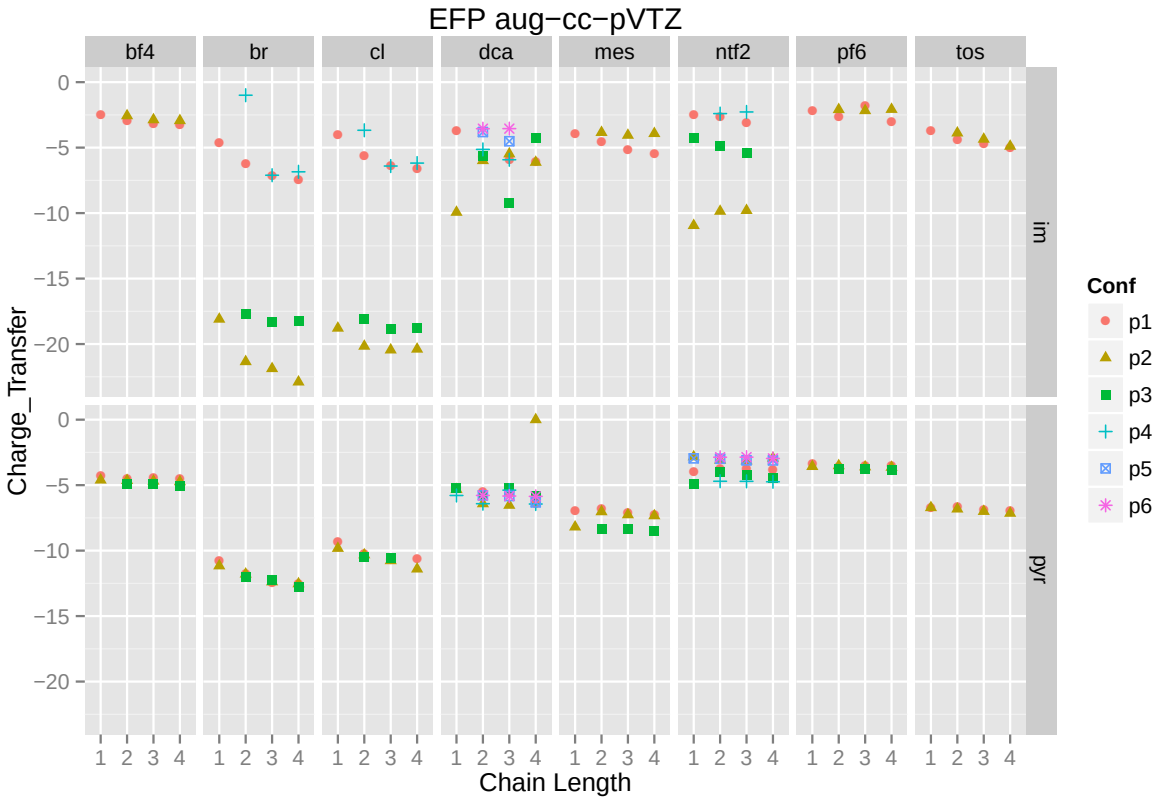

Figure 20: EFP Charge-transfer Energy

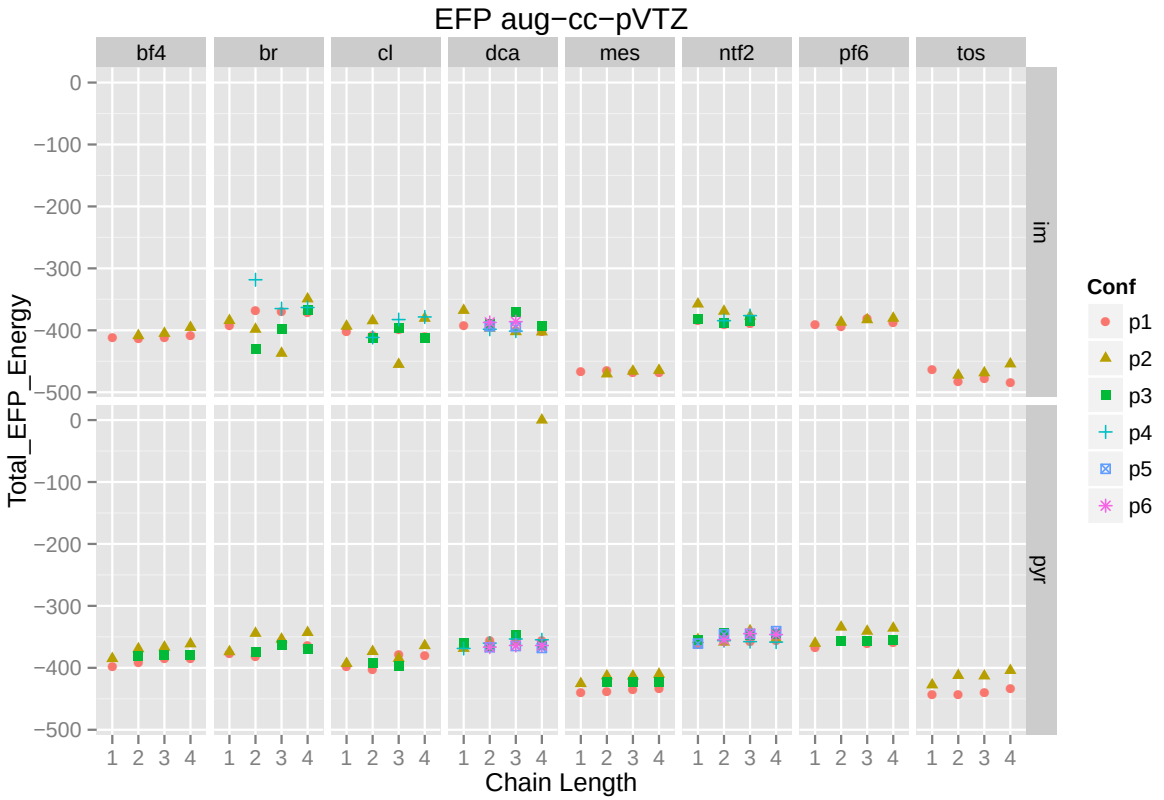

Figure 21: EFP Total Energy

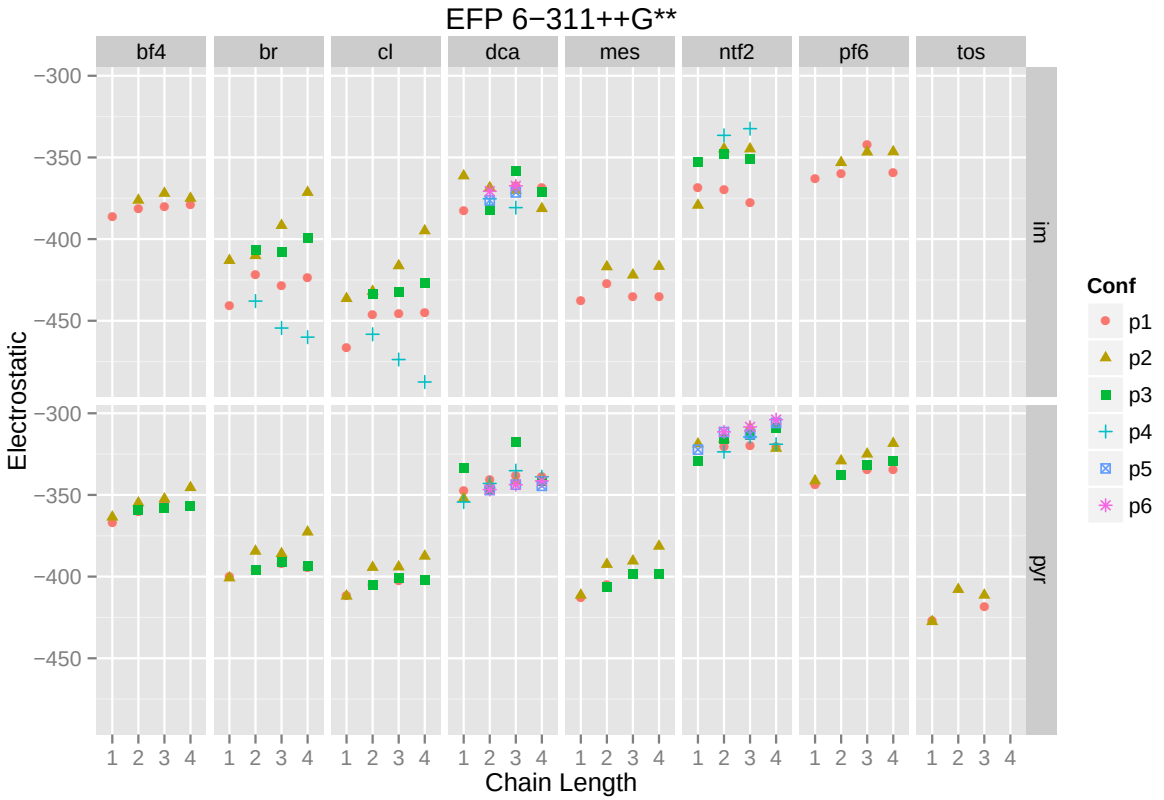

Figure 22: EFP Electrostatic Energy

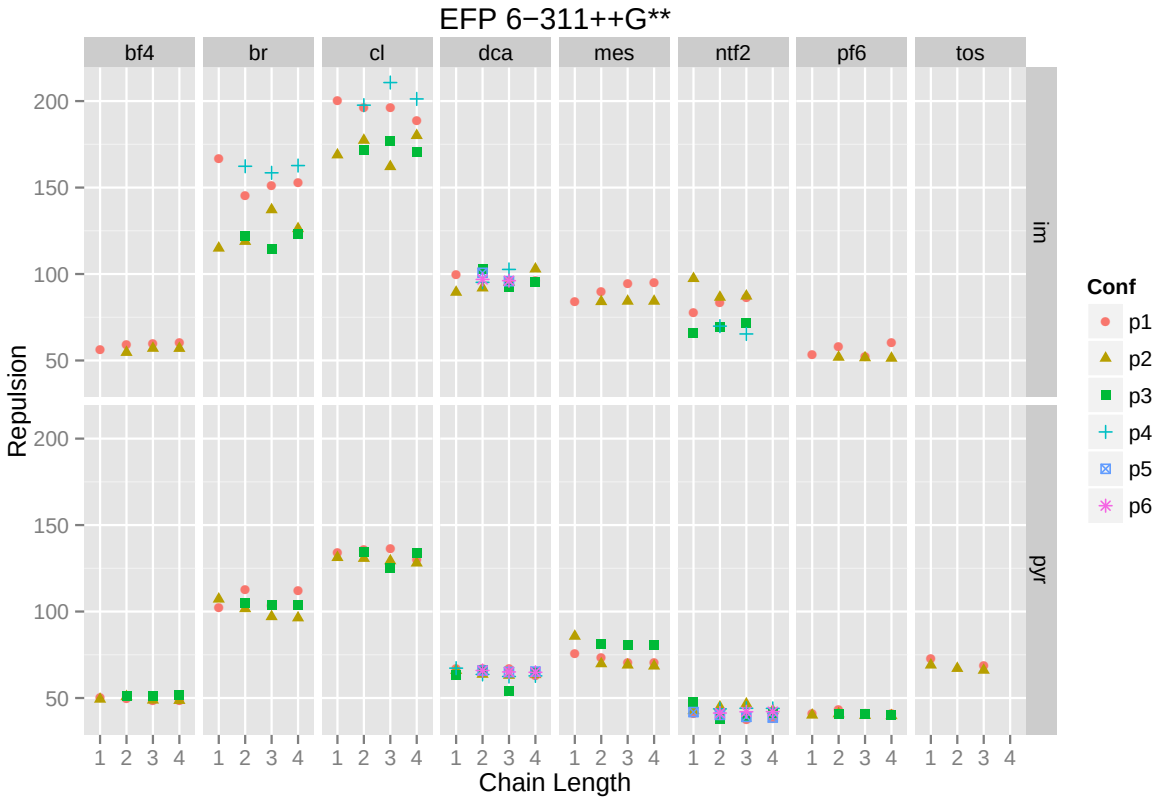

Figure 23: EFP Repulsion Energy

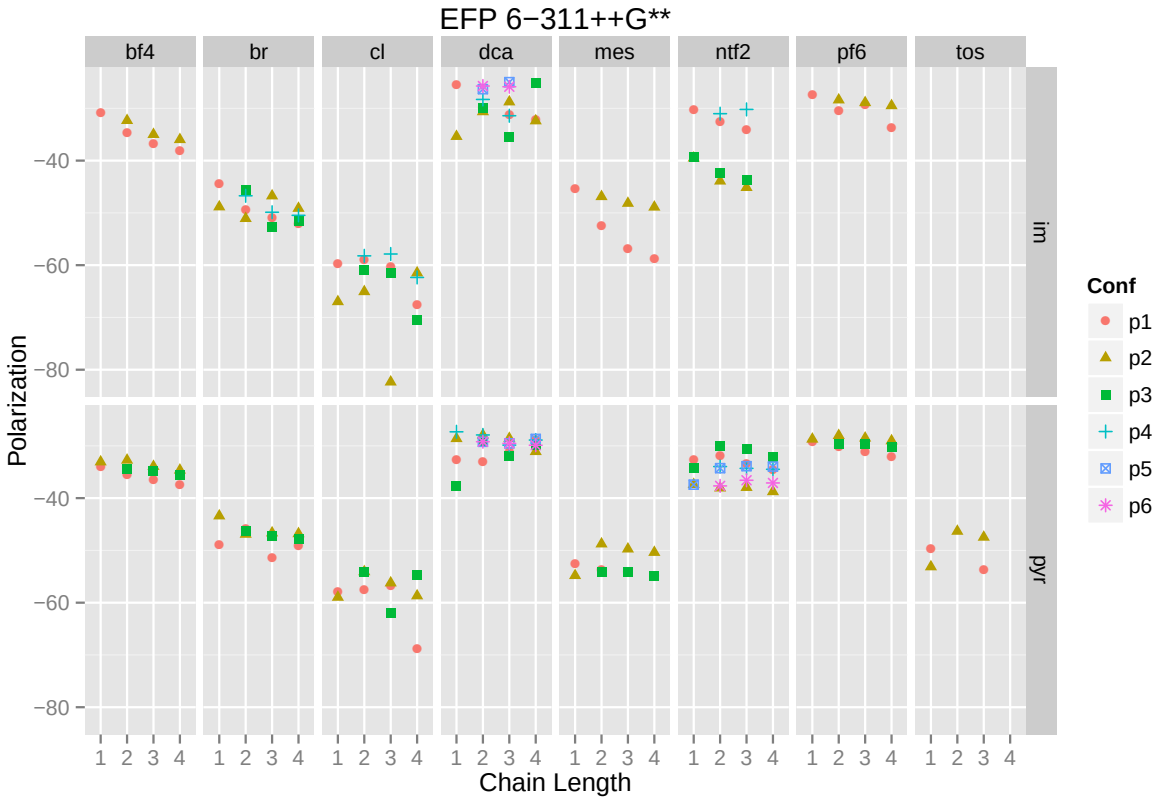

Figure 24: EFP Polarization Energy

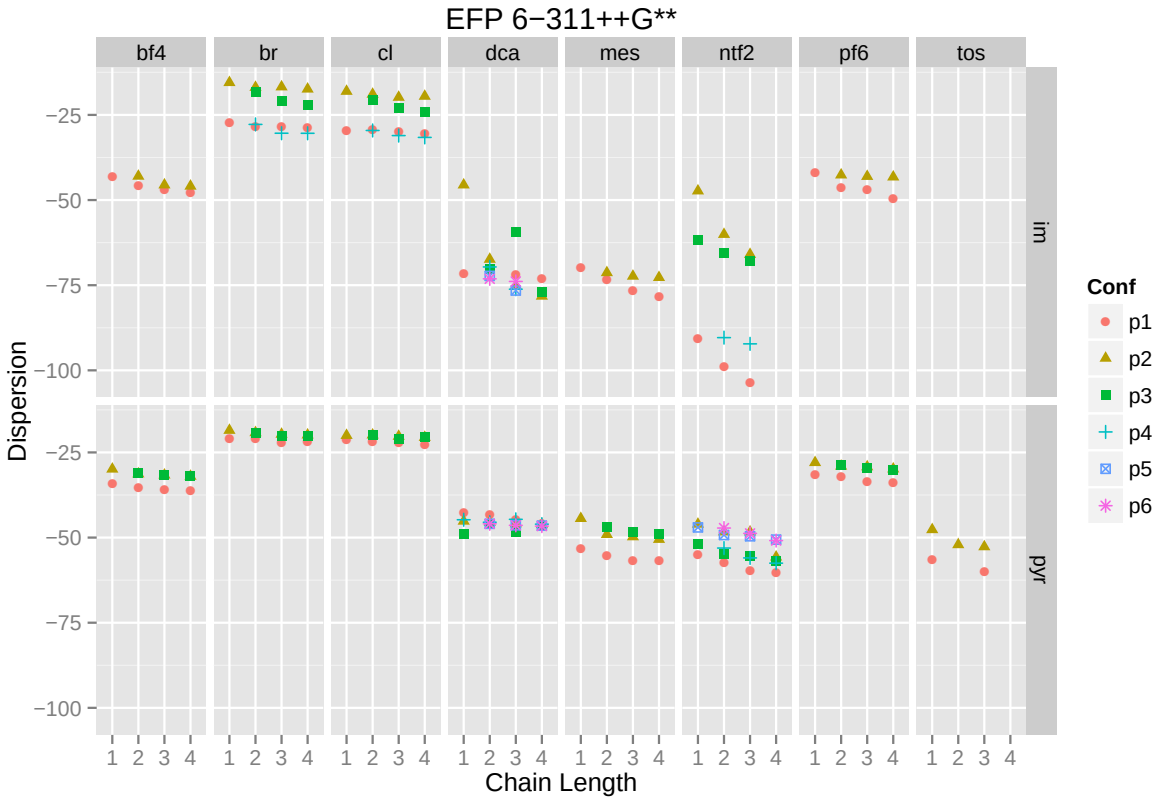

Figure 25: EFP Dispersion Energy

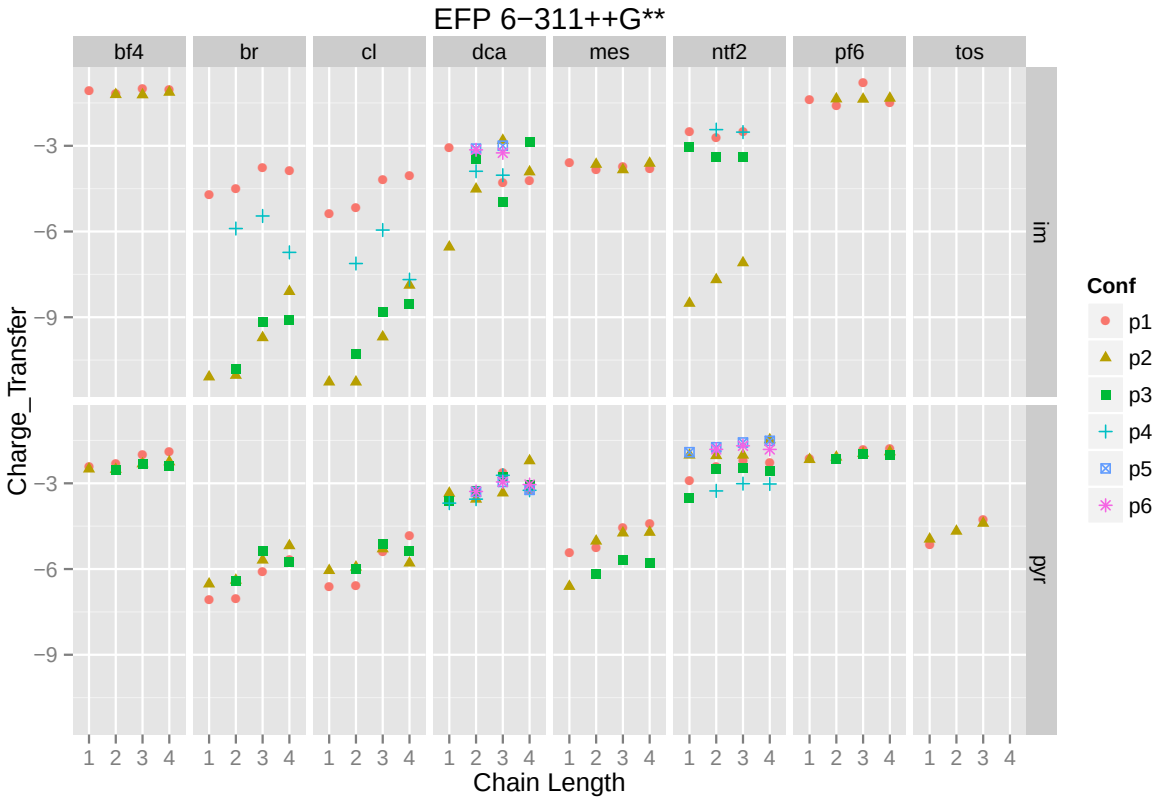

Figure 26: EFP Charge-transfer Energy

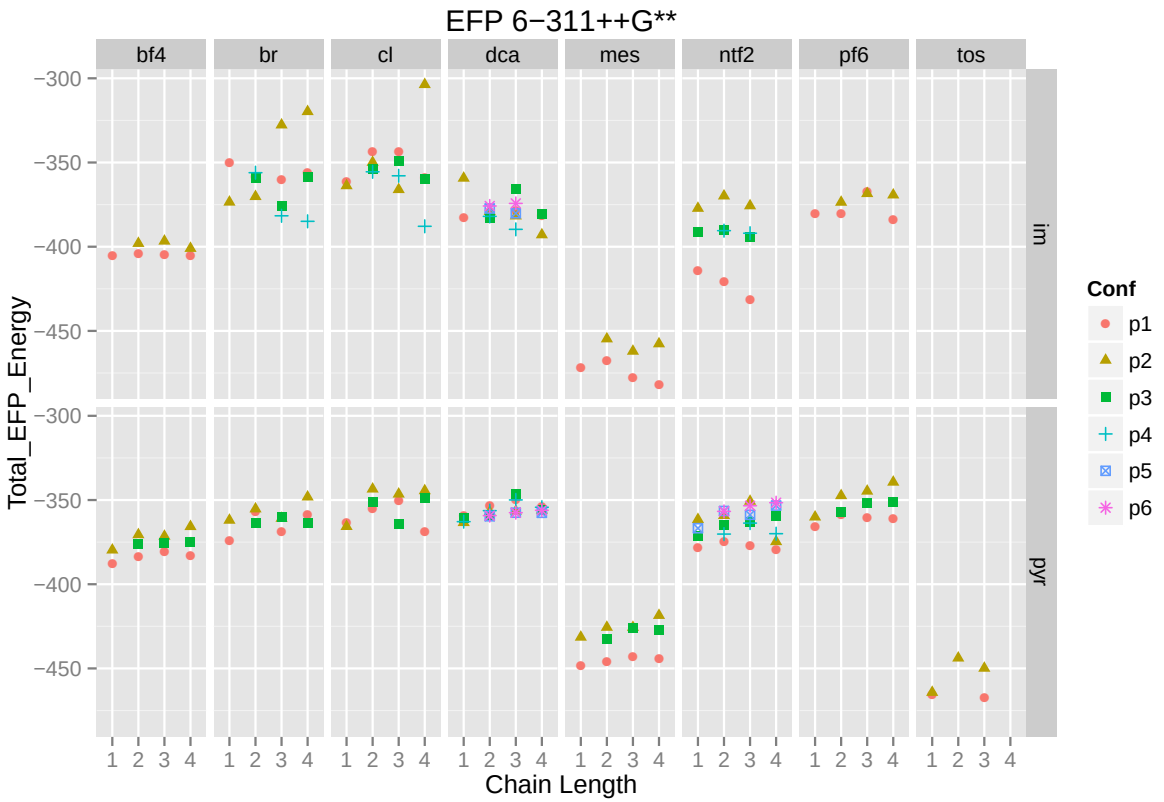

Figure 27: EFP Total Energy

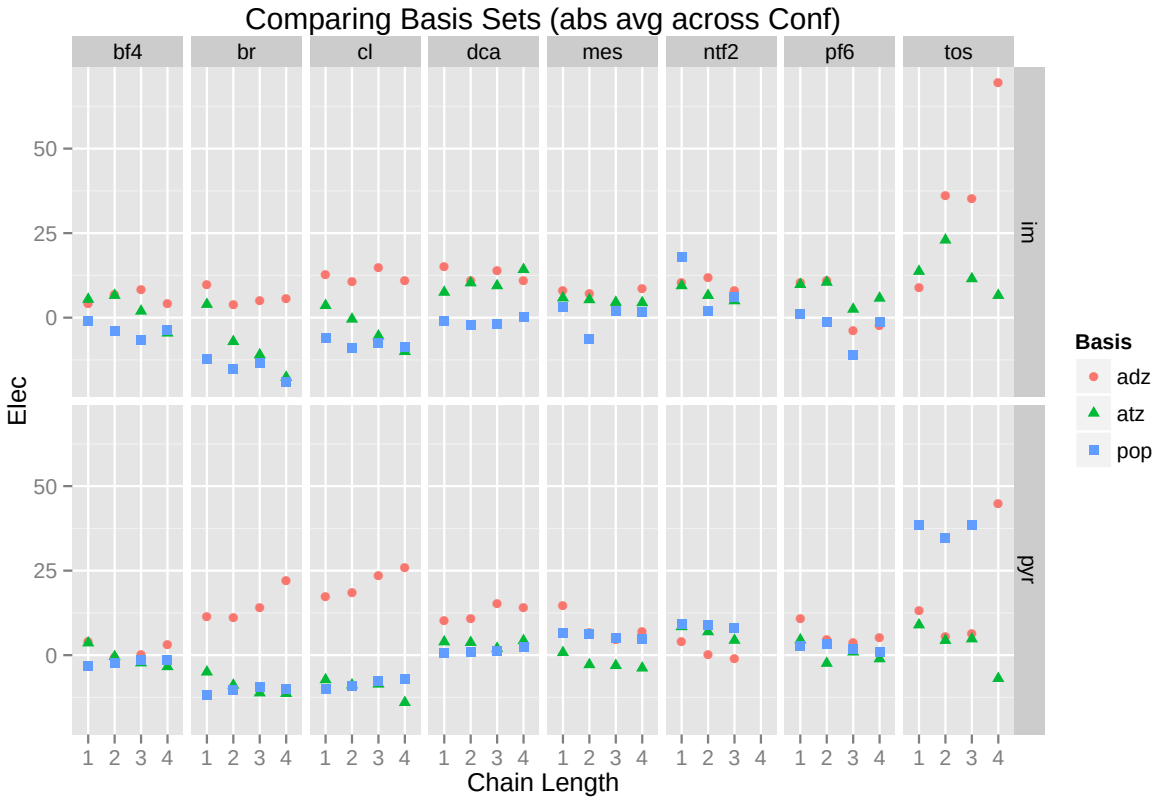

Figure 28: Absolute error for Electrostatics between the different basis sets

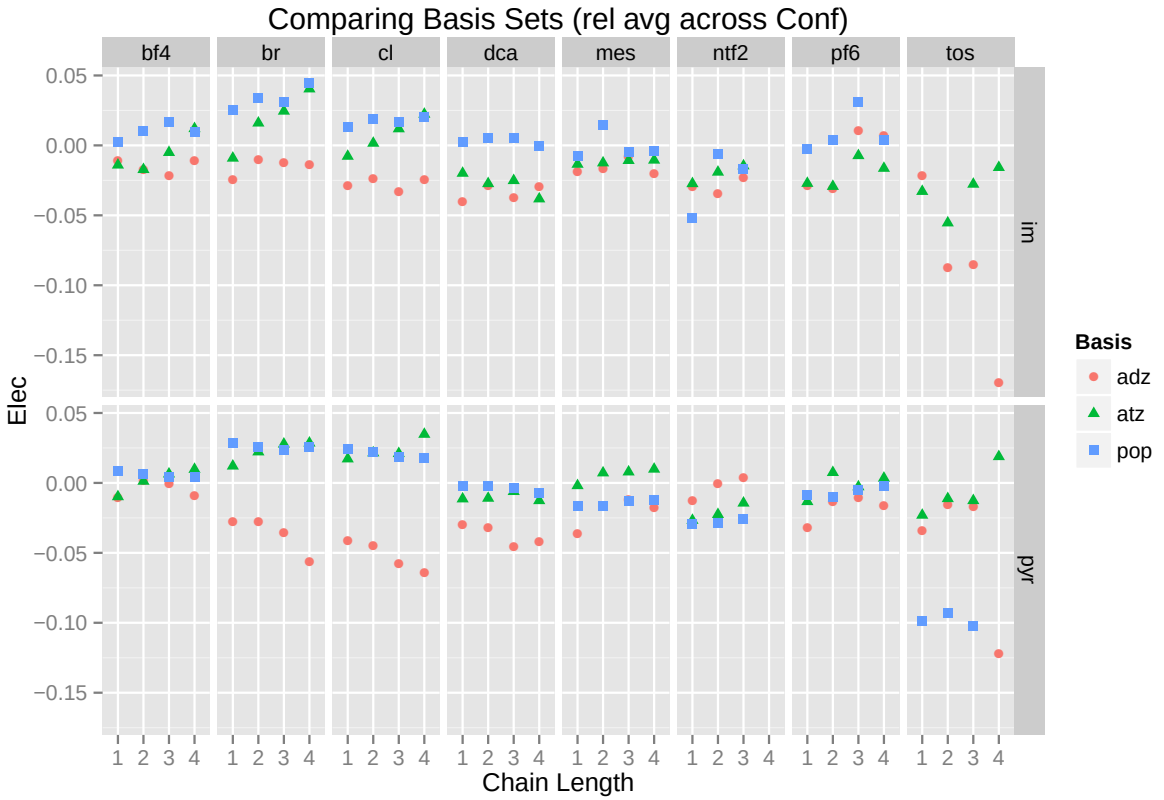

Figure 29: Relative error for Electrostatics between the different basis sets

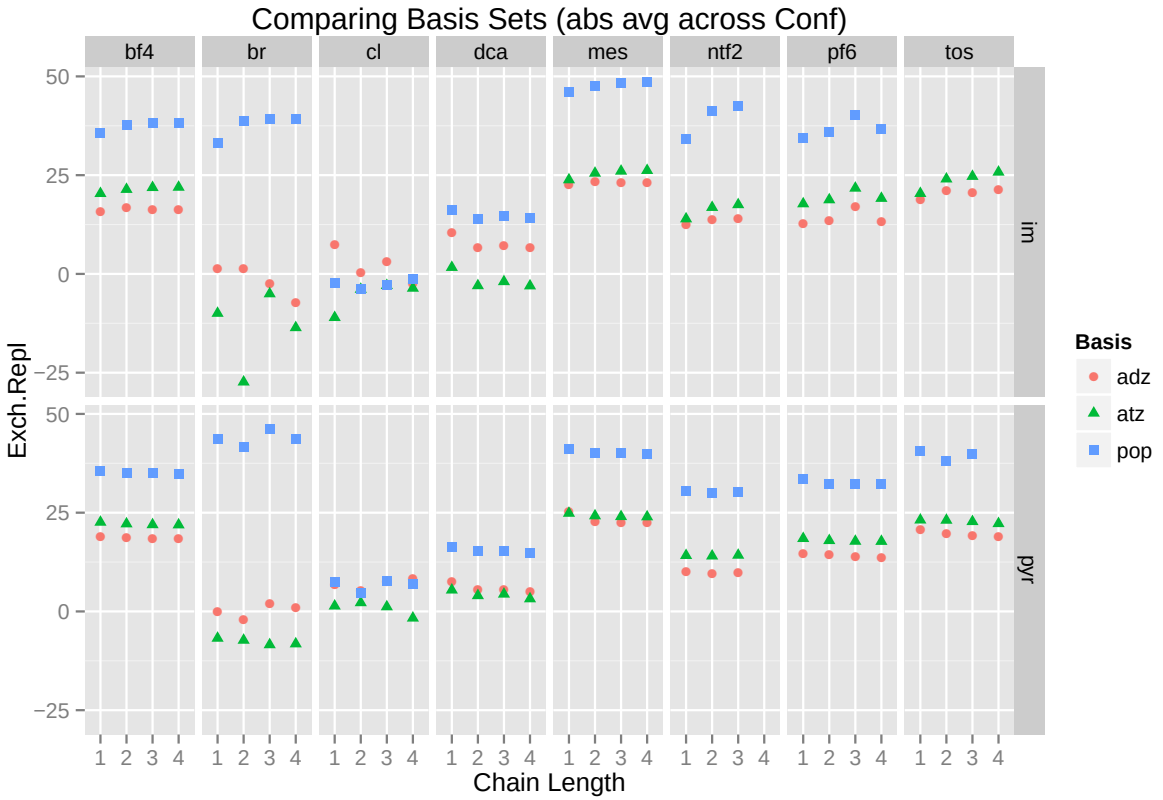

Figure 30: Absolute error for Exchange-Repulsion between the different basis sets

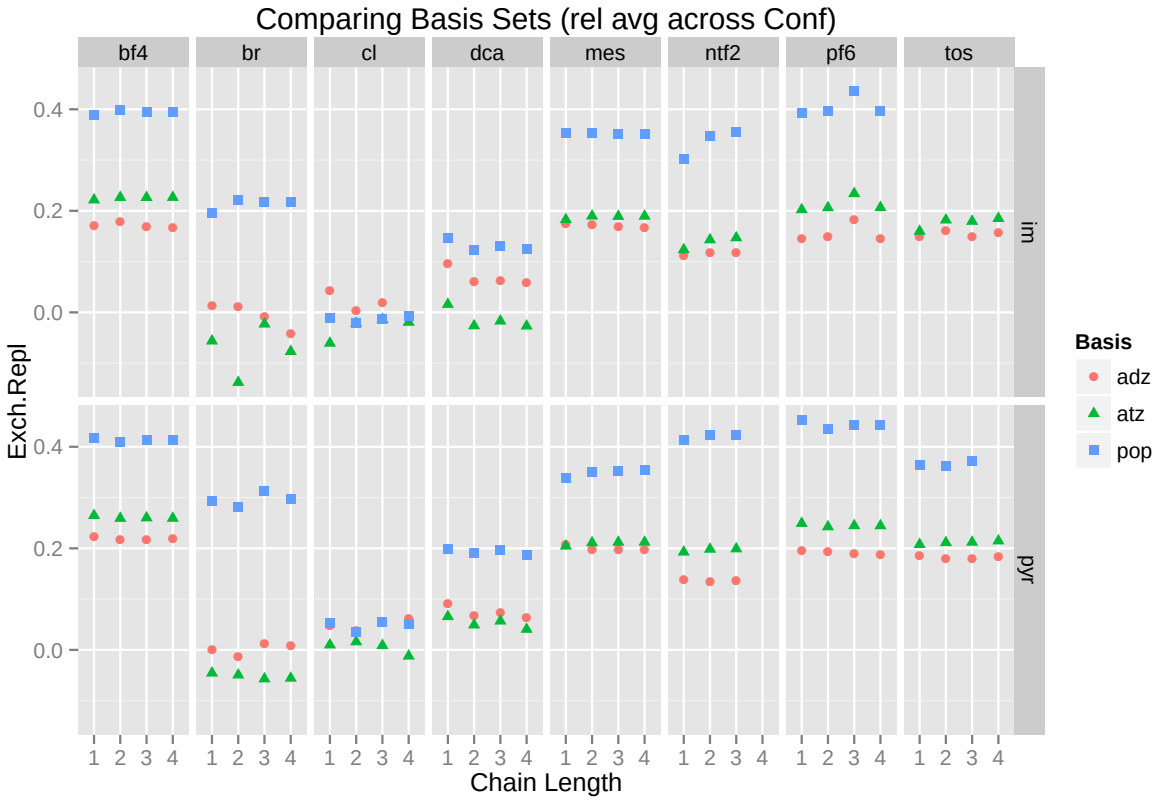

Figure 31: Relative error for Exchange-Repulsion between the different basis sets

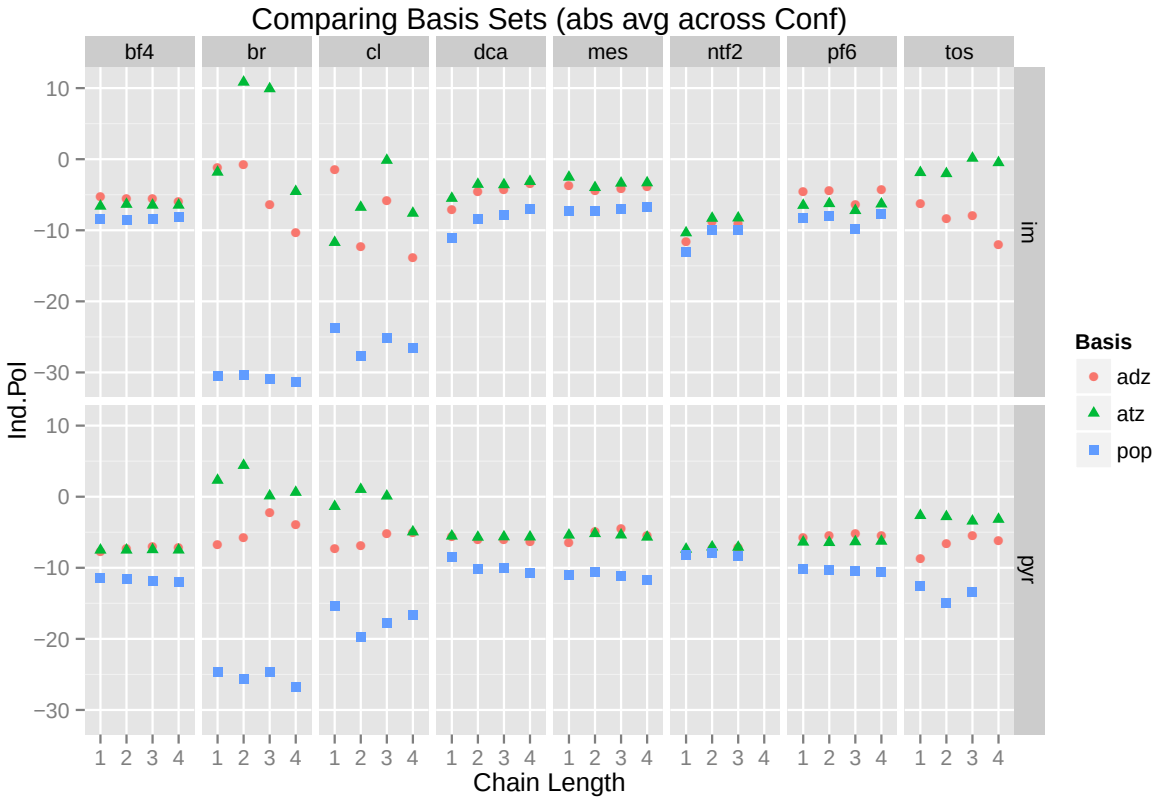

Figure 32: Absolute error for Induction-Polarization between the different basis sets

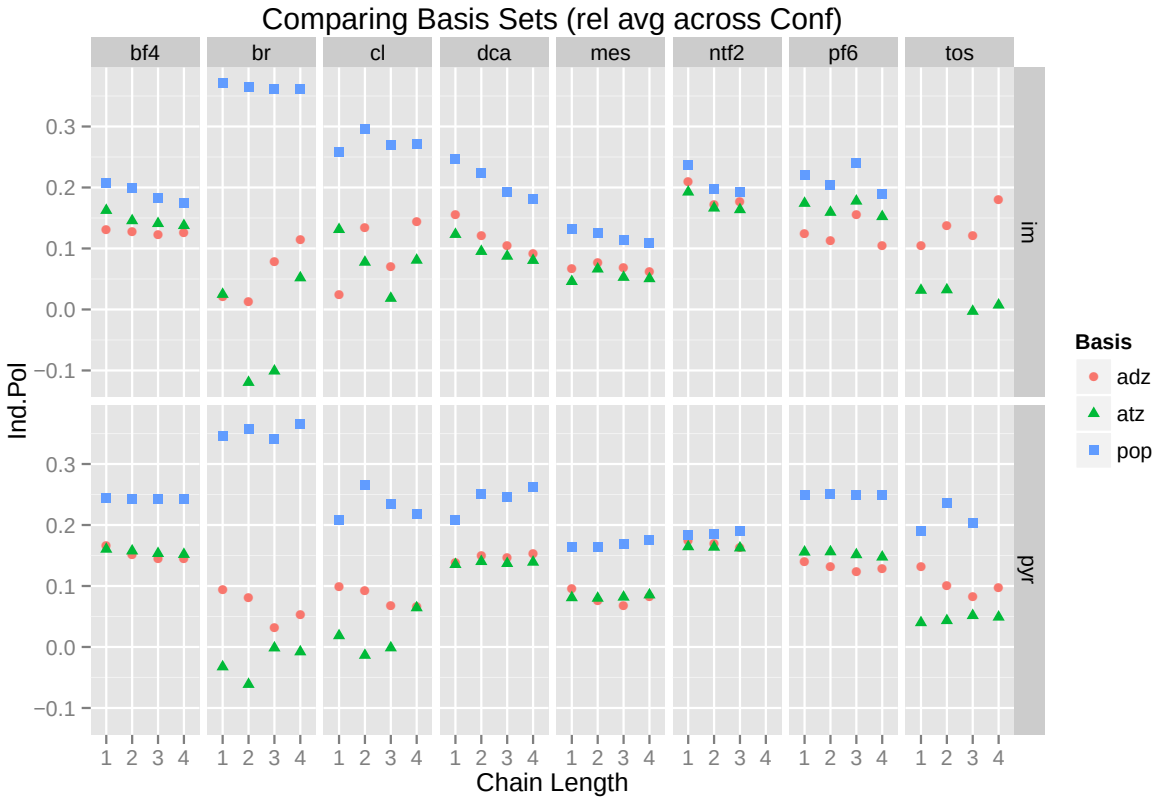

Figure 33: Relative error for Induction-Polarization between the different basis sets

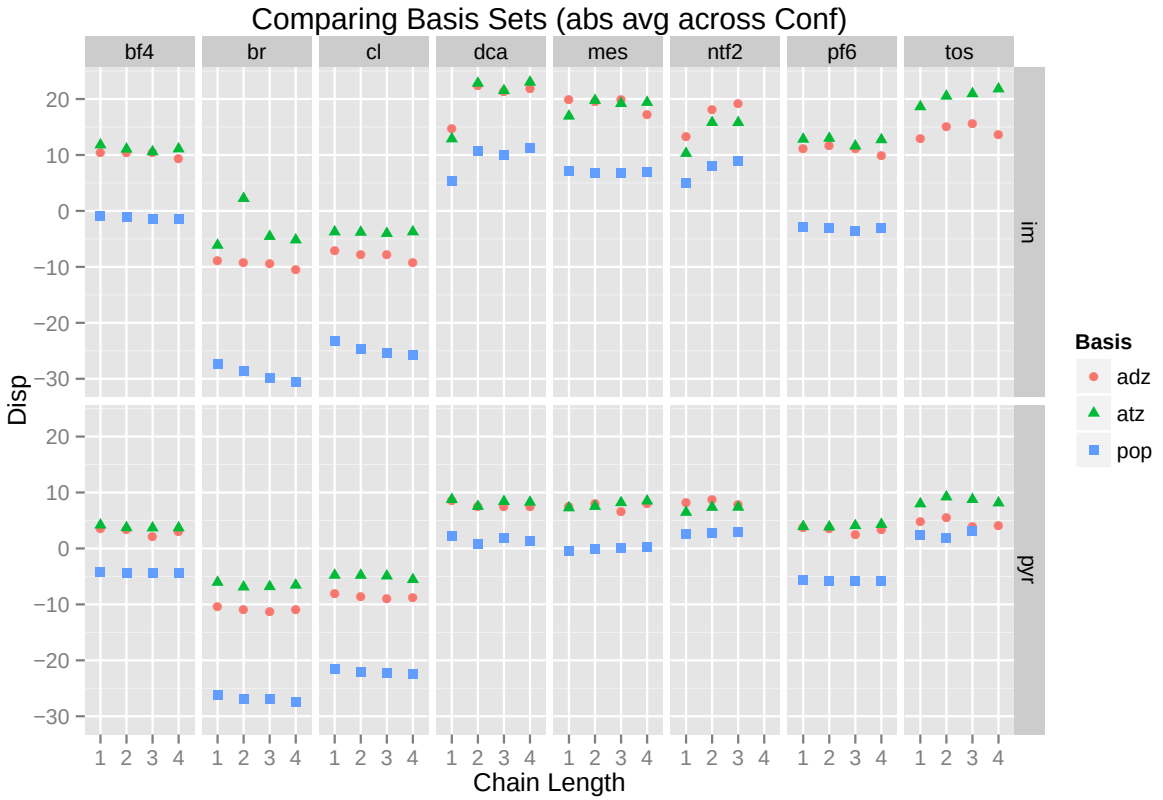

Figure 34: Absolute error for Dispersion between the different basis sets

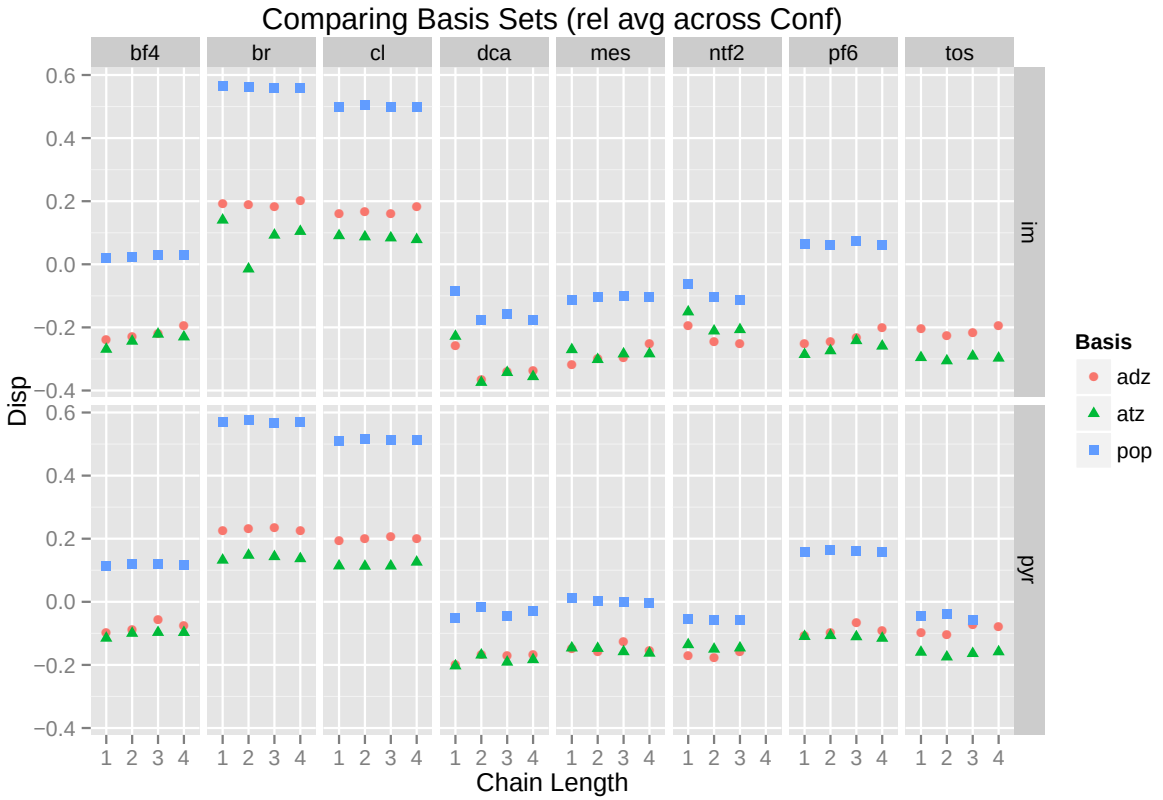

Figure 35: Relative error for Dispersion between the different basis sets

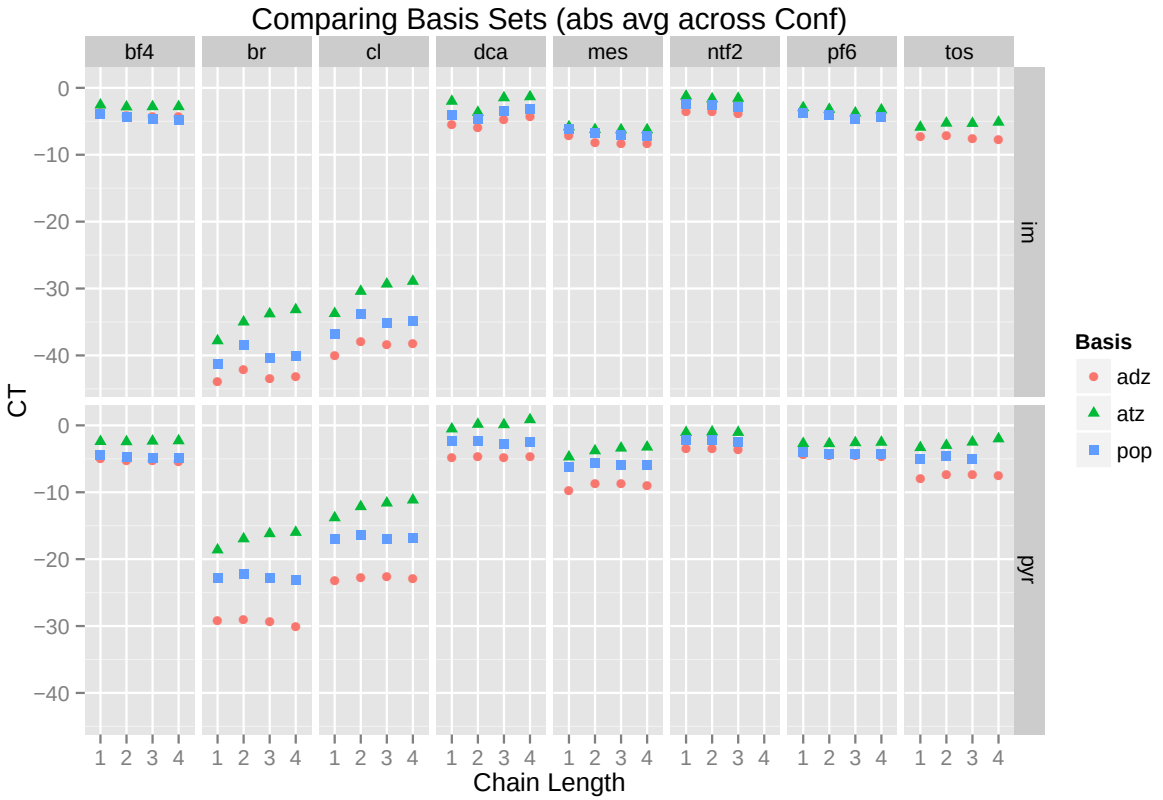

Figure 36: Absolute error for Charge-transfer between the different basis sets

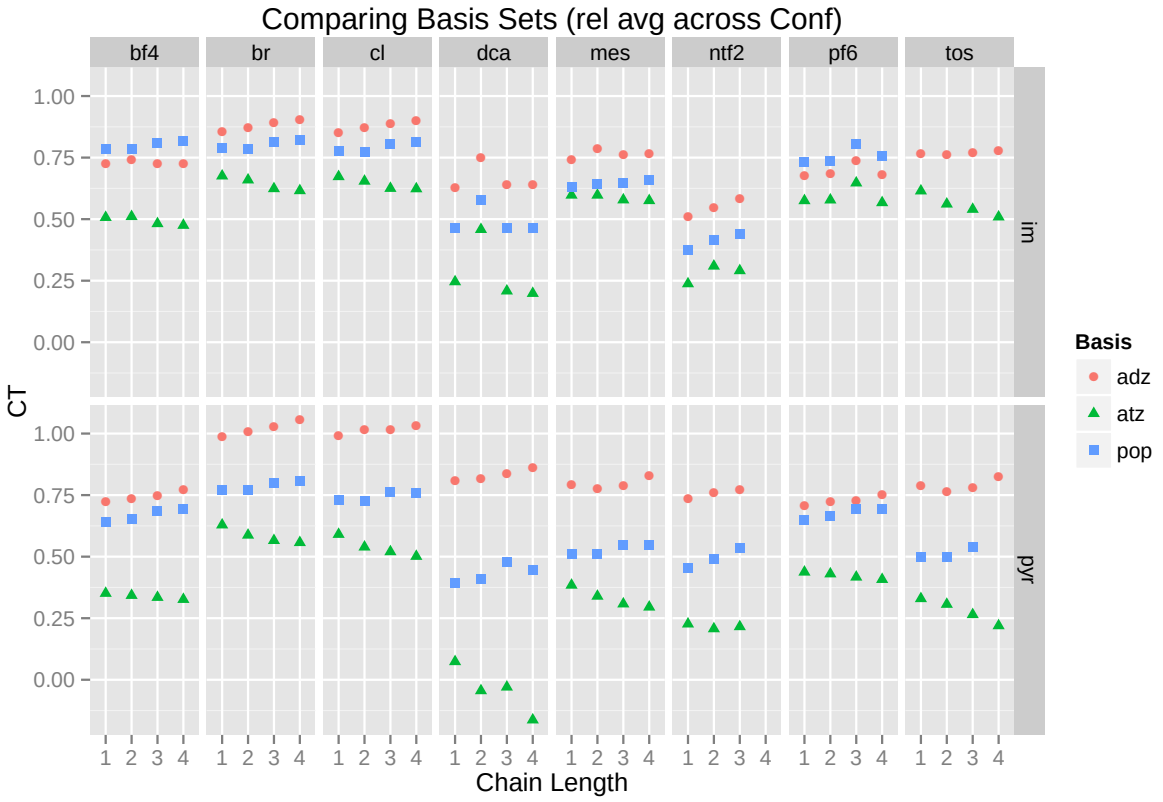

Figure 37: Relative error for Charge-transfer between the different basis sets

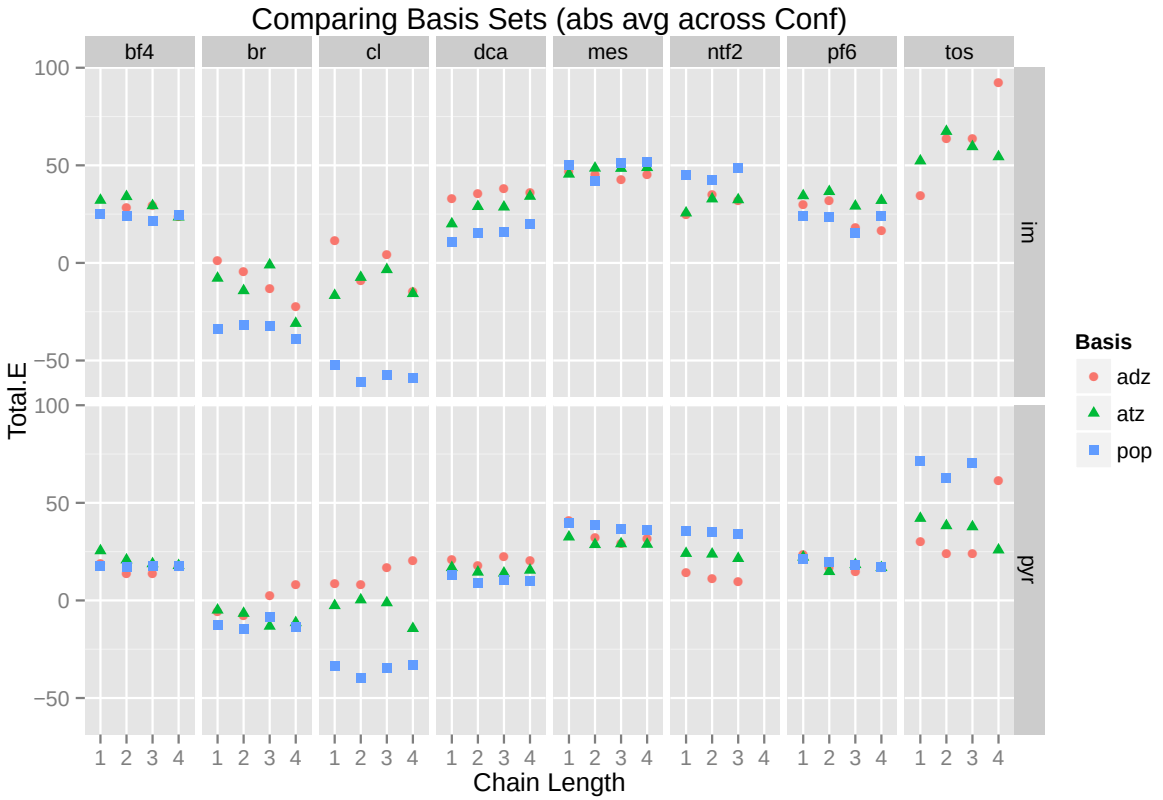

Figure 38: Absolute error for Total Energy between the different basis sets

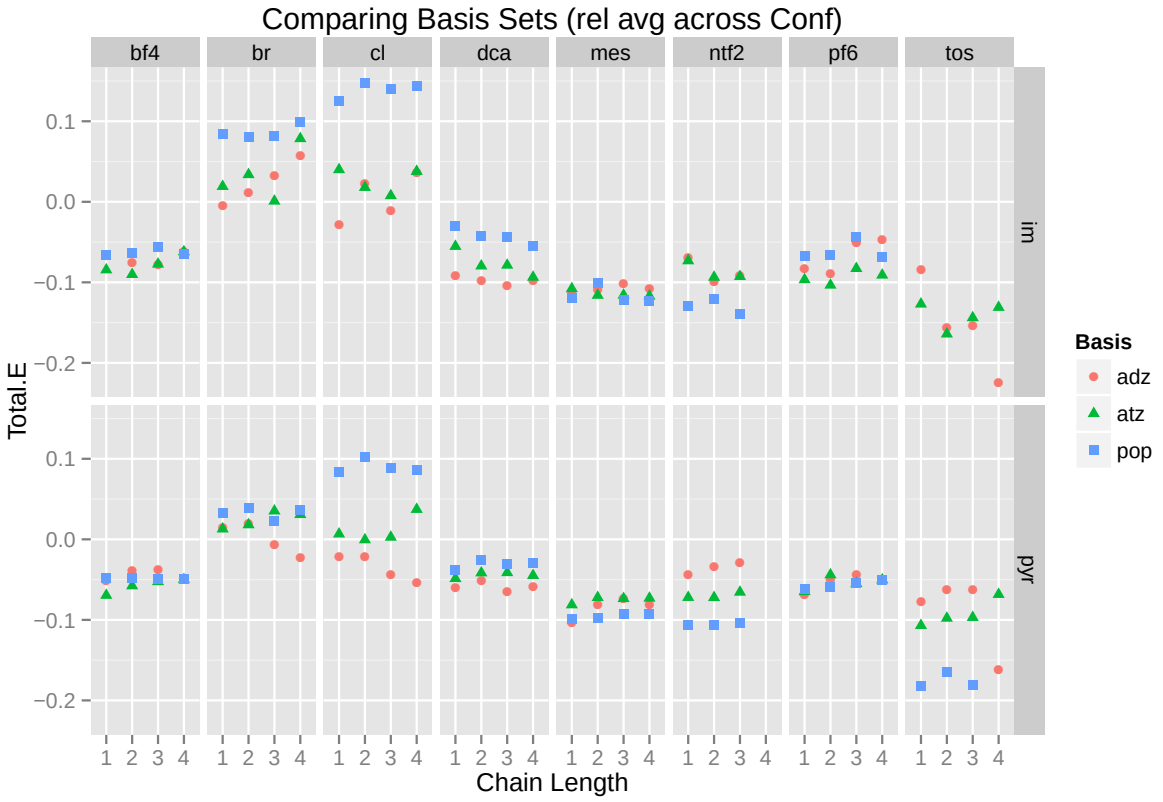

Figure 39: Relative error for Total Energy between the different basis sets

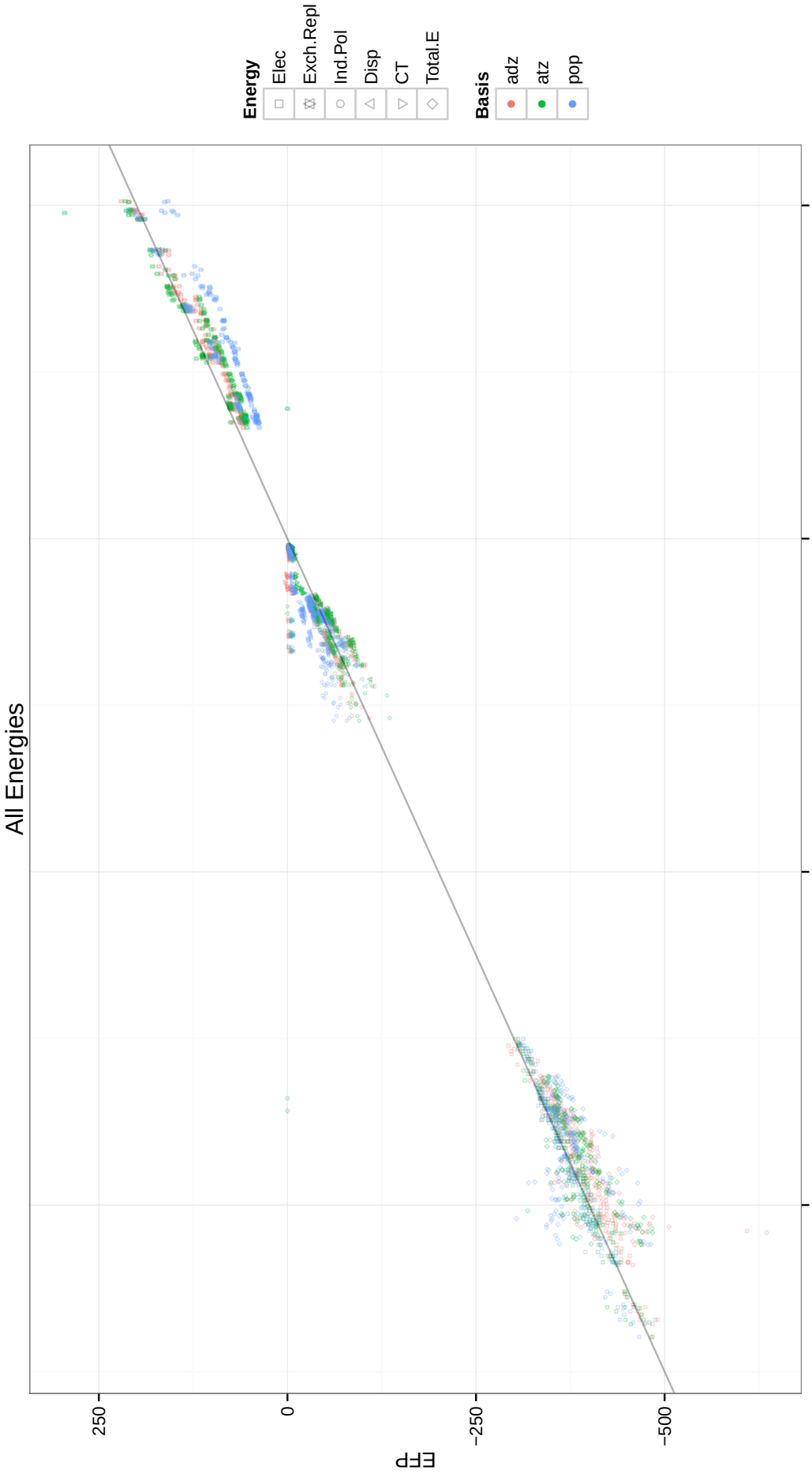

Figure 40: Correlating SAPT and EFP across all energies comparing basis sets

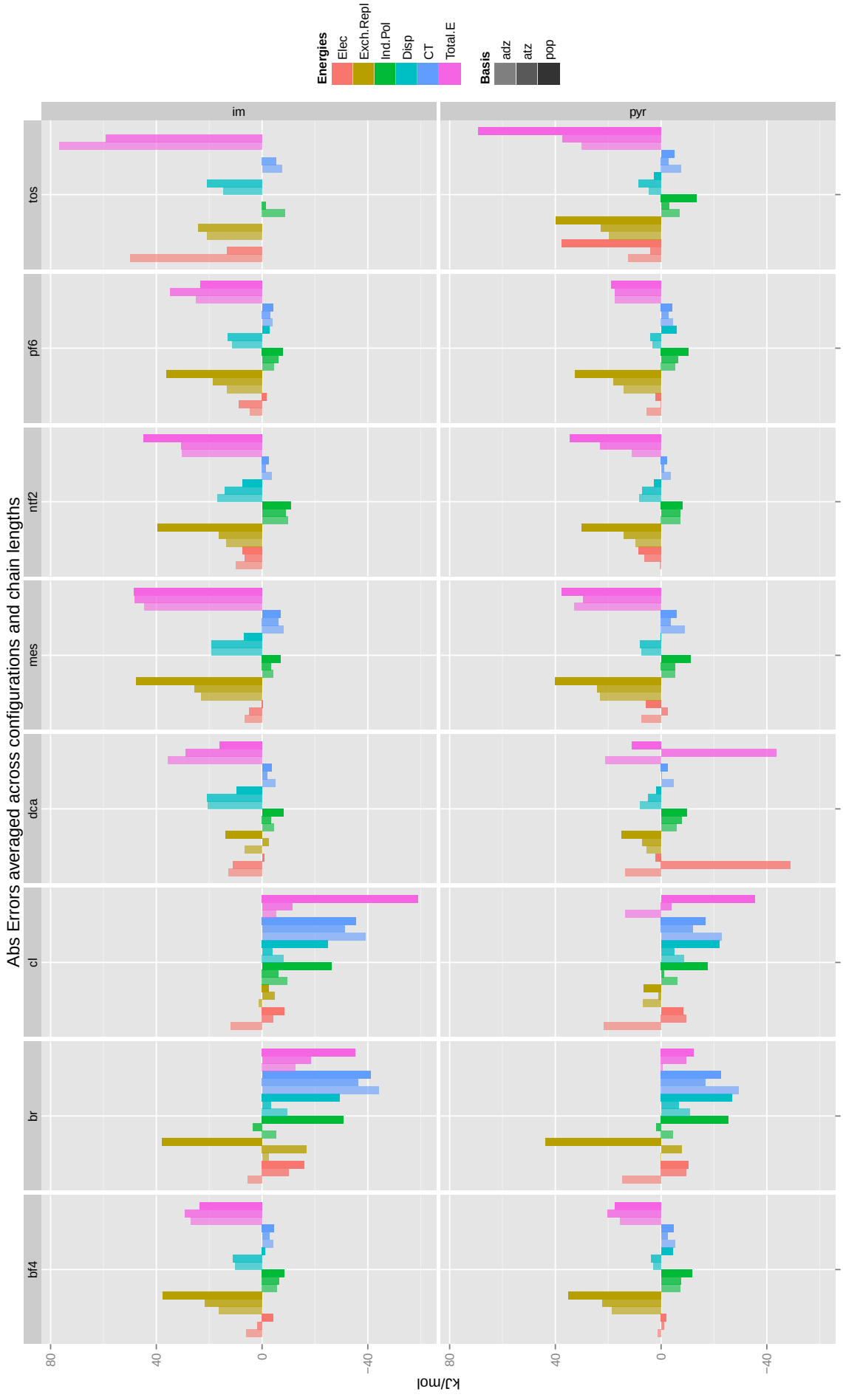

Figure 41: Errors from the different energy components and basis sets used, averaged across configurations and alkyl chain lengths

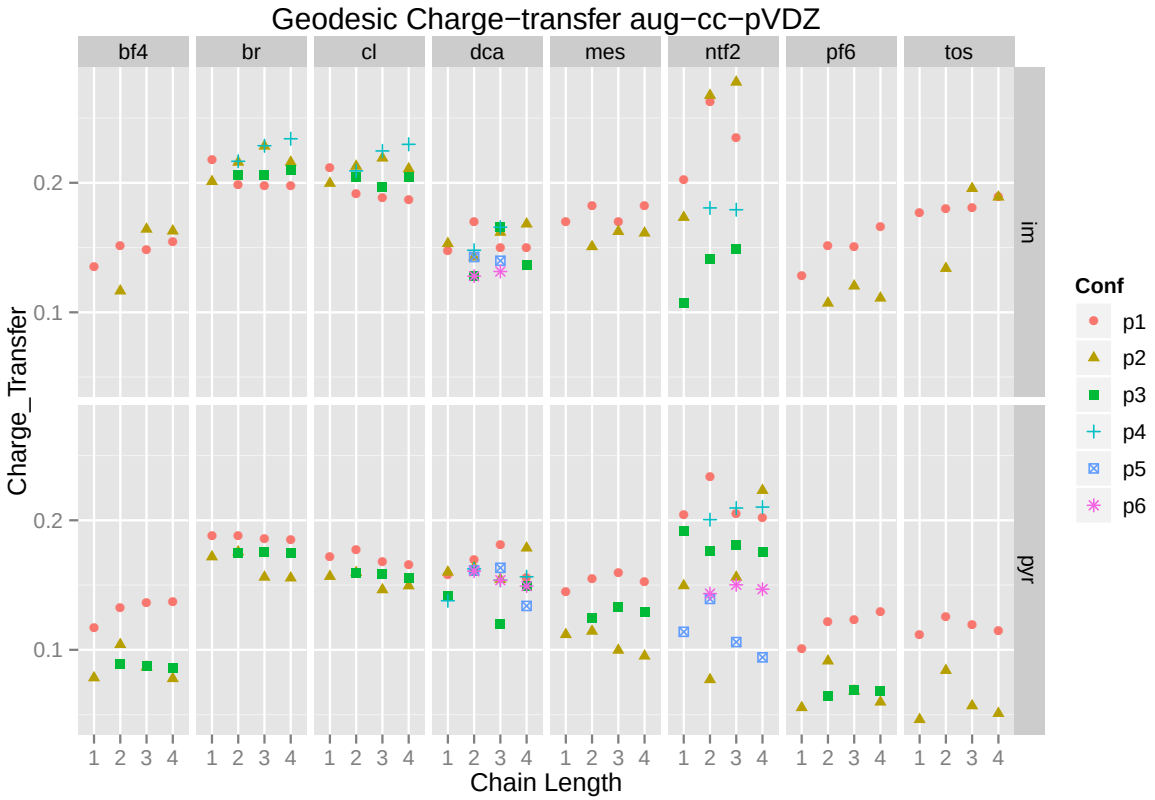

Figure 42: Charge-transfer from geodesic scheme, double zeta

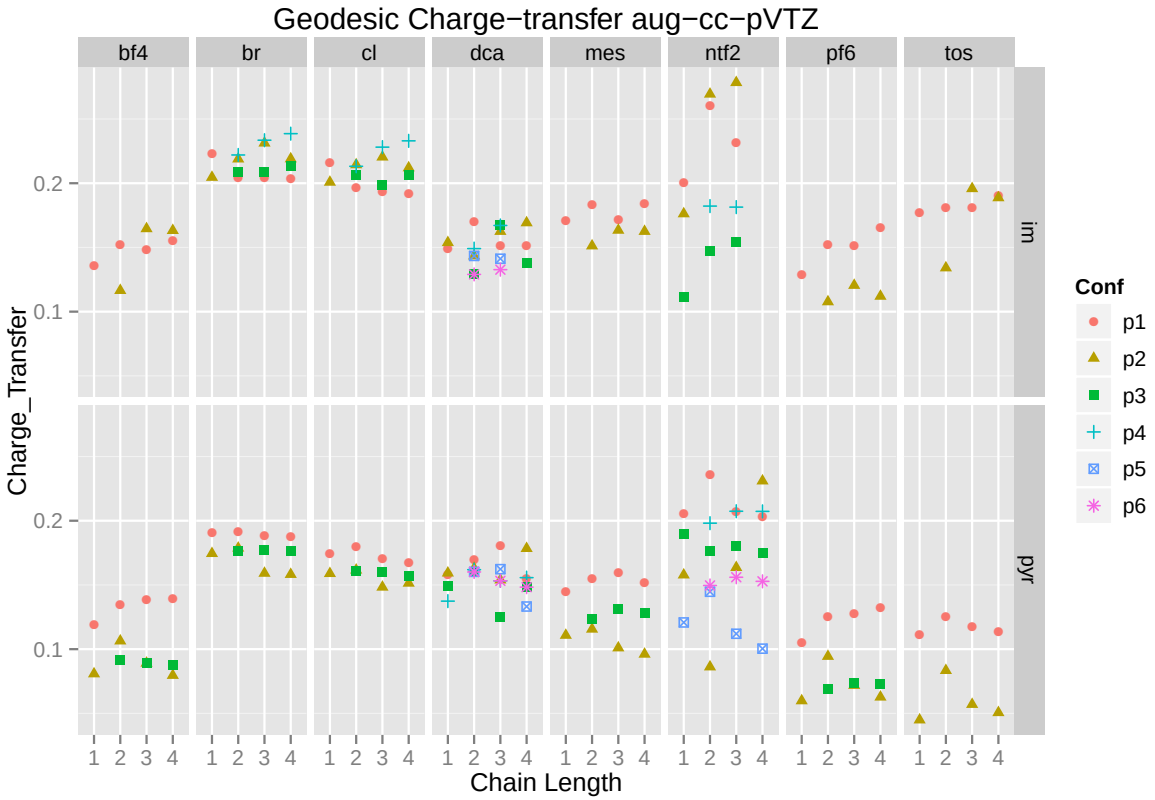

Figure 43: Charge-transfer from geodesic scheme, triple zeta

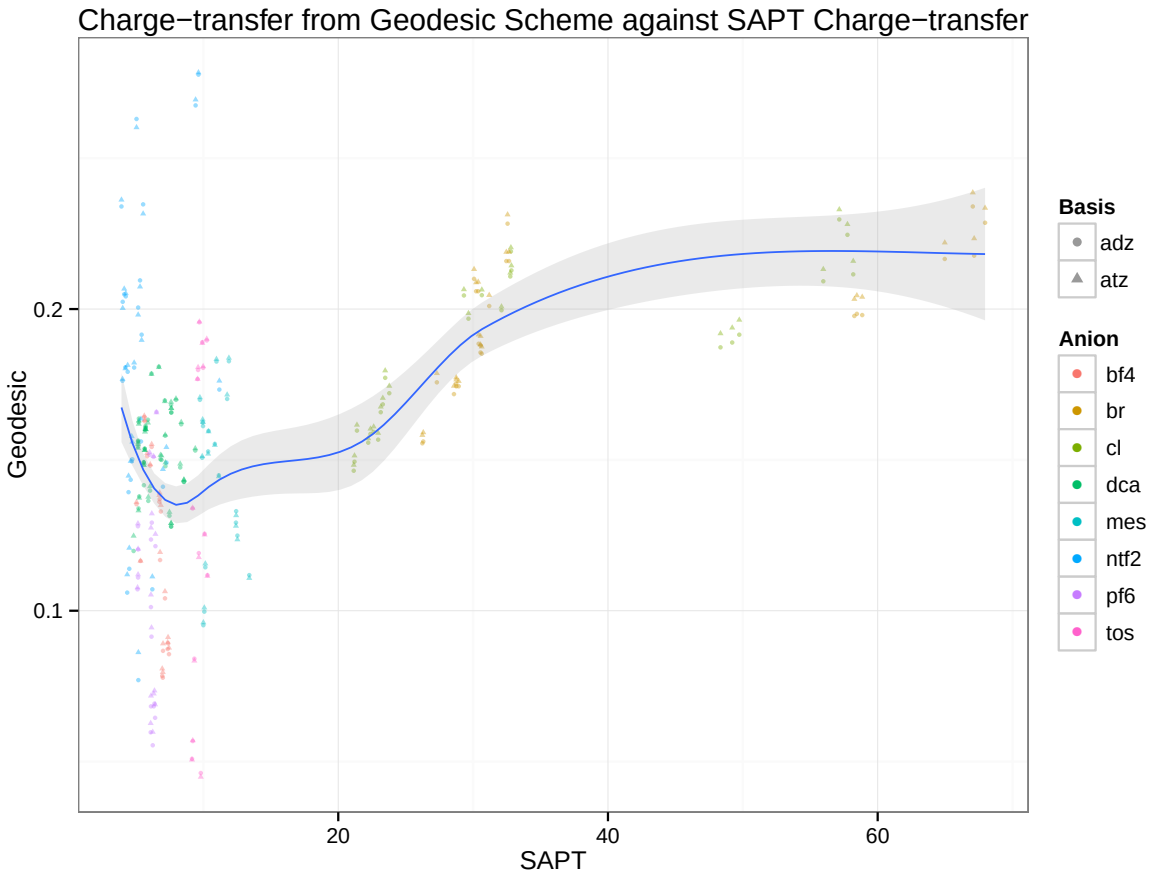

Figure 44: Correlation scatterplot of the charge-transfer from the geodesic scheme against the charge-transfer energy calculated from SAPT